Financial viability analysis of workplace charging using an agent-based modelling approach

Sebastian Lange[1,2,3], Dominic Goh[1,2], Peter Sokolowski[1], Mahdi Jalili[1], and Xinghuo Yu[1]

[1]*School of Engineering, RMIT University, 124 La TrobeSt, Melbourne, 3000, VIC, Australia*

[2]*Authors contributed in equal parts*

[3]*Corresponding author. Email: s3739258@student.rmit.edu.au*

October 26, 2021

Abstract

The widespread adoption of electric vehicles requires an extensive charging infrastructure ranging from private to public solutions. Charging stations located at workplaces are projected to grow in numbers and can take advantage of employees' long parking duration. As electric vehicle users might be exposed to numerous charging options with various associated costs, competitive pricing of workplace charging will be imperative for long-term financial viability. This paper presents an economic framework which utilises a price-signal driven agent-based approach to model the interconnected interactions between electric vehicles and various charging sources. Moreover, a risk-sensitive charging strategy is proposed which minimises charging costs by increasing residential photovoltaic self-consumption. Our findings indicate that changes in preferred charging sources are driven by workplace charger availability and pricing. Additionally, the long-term revenue generation potential of workplace chargers is shown to be affected by the penetration level of residential photovoltaic across the population.

Keywords: Electric vehicles, agent-based model, workplace charging, photovoltaic, cost optimization.

1 Introduction

Nearly a quarter of direct CO_2 emissions from global fuel combustion can be attributed to the transport sector (IEA, 2020). Transport electrification has the potential to reduce greenhouse gas emissions through the use of electric vehicles (EVs) (Knobloch et al., 2020; Bosetti and Longden, 2013). As an alternative to conventional fossil fuelled internal combustion engines, EVs can be utilised to decarbonise the transport sector depending on the sources of electricity generation (Kalghatgi, 2018; Pietzcker et al., 2014; Millo et al., 2014). However, the uptake rate of EV technology has been hindered by concerns regarding range, high upfront costs and availability of charging infrastructure (Matthews et al., 2017; Coffman et al., 2017; Nilsson and Nykvist, 2016). Whilst some barriers for EV adoption can be overcome by policy incentives, several issues relating to charging have yet to be addressed (Langbroek et al., 2016; Lieven, 2015). Most noticeably, the effects of large-scale use and reliance of workplace charging have yet to be explored.

1.1 Background

Whilst there is growing interest in EVs, electric cars only accounted for 2.6% of global car sales in 2019 (IEA, 2019). Due to the low market share of EVs, academic literature regarding consumer interaction with EV charging infrastructure on a large scale has been limited. The importance of home, work and public chargers vary according to consumer access. Home charging has been identified as the primary source of recharging EVs and the most crucial element of charging infrastructure required for widespread EV adoption (Hardman et al., 2018; Bailey et al., 2015). The second most frequent charging location after home charging is the workplace. This is in line with daily human mobility patterns derived from surveys and mobile phone data where the most common behaviour

consists of travel between two locations (Schneider et al., 2013). While workplace charging may not become the primary charging source, projections for the coming decade have shown that work place charger installations will grow substantially in numbers (IEA, 2021). Commuters with no access to home charging will require a regular workplace charger as an alternative option. Public charging stations serve a similar role for substituting home charging for those with limited availability, despite being the least frequently used location for charging overall (Funke et al., 2019). The charging behaviour observed from early trial projects indicate that consumers are motivated by convenience (Azadfar et al., 2015). However, these trials involved a small EV sample size and financial incentives such as free charging. The transition from early adopters to widespread EV users will likely change the interdependency of home and workplace charging infrastructure.

The long-term financial viability of workplace charging will depend on numerous variables. Upfront capital expenditure will be required for the initial installation of workplace charging infrastructure. This can include the costs associated with design, site provisions, hardware components and cost of labour. Moreover, variation in expenditure is expected depending on the power level and number of chargers installed (Nicholas, 2019). However, the long-term financial viability will be dependent on the operation phase of workplace chargers where ongoing costs will also be incurred for electricity usage, network charges and maintenance. Electricity utility charge can be associated with either peak continuous power used or amount of energy used. In the latter case, the metered total consumption will be based on the amount of energy required by employees. The amount an EV requires is inherently linked with the distance commuted by the user. Subsequently, the employer is subjected to uncertainties associated with utilisation of workplace chargers which serves as a method for cost recovery. As such, there are several works on the economic feasibility of workplace charging. An optimisation framework for workplace charging strategies was proposed where average national data was used to demonstrate the applicability and generality of the methodology (Huang and Zhou, 2015). Workplace charging lifetime costs were minimised whilst all charging demand of EVs were satisfied by the strategy provided by the general decision-making framework. Whilst the employees' energy needs

were met, competition introduced by alternative sources of charging was not included. Electricity mark-up was the main focus of another study which included the consumer perspective where electricity prices were compared to gasoline prices (Williams and DeShazo, 2014). This included benchmarks comparing different proposed pricing structures with varying degrees of cost recovery in addition to a break-even pricing scenario. A sensitivity analysis was included to account for electricity cost fluctuations, but similarly did not include the possibility of access to alternative charging sources such as home or public charging. Conversely, a comprehensive model which included both the employer's and employee's perspectives was presented in another study (Fetene et al., 2016). Several workplace charging contract schemes were proposed with different utility focuses, including a joint perspective scenario. Whilst numerous parameters were included to reduce the number of uncertainties involved, the possibility of employees having access to a residential photovoltaic (PV) array installed along with their home charger was not included. In recent years, the cost of PV systems have reduced significantly (Feldman et al., 2021). Consequently, increased rooftop PV installations has resulted in Australia having the highest uptake globally (Cranney, 2021). The inclusion of residential rooftop PV at an employee's home charger will subsequently introduce uncertainties to workplace charger utilisation where employers will be subjected to the risk associated with this variable.

The concept of electricity consumption at the same time as PV generation is known as self-consumption and has been previously explored in the context of household loads (Bhandari and Stadler, 2009). However, recently this concept has been extended to include EV charging and even the inclusion of vehicle-to-home technology. This was the main focus of a paper which found that households with long EV absence times proved to be more economical when a vehicle-to-home system was combined with a stationary battery (Higashitani et al., 2021). However, in general the installation of a vehicle-to-home system instead of a stationary battery was found to be more profitable in some scenarios. Similarly, another study focused on EV charging in the presence of PV generation without the inclusion of additional energy storage systems. A deep reinforcement learning approach was utilised to optimise for increased PV self-consumption and EV state-of-charge at

departure (Dorokhova et al., 2021). In both studies, external factors such as the possibility of exporting electricity generated from PV or charging infrastructure exclusive of home charging were not considered. Alternatively, another paper focused on how self-consumption could be implemented in the context of workplace charging instead of home charging (van der Meer et al., 2018). This was achieved through the use of a proposed energy management system that utilised an autoregressive integrated moving average model to predict PV generation and a mixed-integer linear programming framework to optimise for minimal charging cost. However, the assumption of a PV installation at the workplace circumnavigates the dilemma where an EV is not present at home; unable to utilise peak PV generation at the residential level. Moreover, the cost minimisation with the inclusion of a feed-in tariff was formulated with a focus of the owner of a workplace parking lot as the main stakeholder where costs incurred by the EV users were not included. As such, the effect of including PV self-consumption at the residential level interconnected with workplace charging from the perspective of EV users has yet to be considered.

1.2 Contributions

The main contributions of this paper are as follows:

1. Proposed an economic framework exploring the cost sensitive nature of charging source preference based on the interconnections of workplace and home charging with the inclusion of residential PV. The objective of this framework is to provide employers with an indication on the financial viability of workplace chargers in the presence of the wider charging infrastructure and cost-sensitive consumers.

2. Utilised a bottom-up approach by designing an agent-based model simulating data-driven travel patterns for commuting to work. This model captures the interaction between consumers and the charging infrastructure on a large scale with the inclusion of both private and public chargers with associated price signals. The provision for PV self consumption was incorporated by modelling household loads in addition

to EV charging loads.

3. The findings show that charging cost variation is driven by changes in workplace charger pricing and demand with the latter being dependent on dwelling types and associated charging infrastructure access.

1.3 Paper Structure

The rest of this paper is organised as follows. Section 2 describes the modelling approach for the agents and environment in addition to the formulation of a risk-sensitive charging strategy designed to minimise charging costs. In Section 3, the simulation results are presented for various scenarios with different stakeholder interests. Section 4 discusses the implications of workplace charging based on the findings in addition to providing directions for future works. Finally, Section 5 concludes the paper with a summary of the main findings.

2 Methodology

This section provides a tool which delivers insight into the effects of a large-scale implementation of work place charging. The utilised approach proposes a price-signal driven agent-based model which is employed in an explorative case study. Agent-based modelling is a technique used to represent a system through a collection of autonomous decision-making entities known as agents. This method utilises a bottom-up strategy to analyse the overall system dynamics that emerge from the collective behaviour patterns of the agents (Bonabeau, 2002). The application of this modelling technique focuses on the operation phase of workplace charging where the design, construction and installation of workplace chargers are considered sunk costs. The mobility patterns and behaviour characteristics of the agents are derived from real-world data where the chosen environment to be emulated is based on metropolitan Melbourne, a region located in Victoria, Australia.

The proposed model can be grouped into three modules which are executed consecu-

tively where an overview is shown in Algorithm 1. First, the model is initialised by setting up an environment for agents to live in (compare Sections 2.1), followed by the creation of n agents (compare Section 2.2). Secondly, the agents interactions are simulated in an iterative process stepping through $\tau_{max} = 4032$ time steps of length $\Delta t = 5$ min $= \frac{1}{12}$ h (compare Section 2.3). In general, the symbol τ is used for time steps, while t denotes time. Lastly, data gathered during the second module's execution is analysed (compare Section 2.4). Executing all three modules consecutively in the mentioned order will be referred to as a run.

The following section outlines how these modules are implemented and configured in the proposed model. Input datasets for these modules in addition to their derivations are further elaborated upon in the appendix section. The proposed model was implemented using Mesa, a Python framework for agent-based modelling (Kazil et al., 2020).

2.1 Initialisation of Environment

Agents operate within a space known as the environment. This can refer to elements such as the built environment or resources which agents can interact with. Subsequently, agents can indirectly interact and affect multiple agents through this shared environment. The proposed model introduces both static and dynamic elements of the environment. For example, the geography such as road networks remain unchanged throughout the simulation whilst seasonal variations introduce fluctuations in potential PV output.

2.1.1 Seasons and weather

The model allows for the selection of one of all four seasons: spring, summer, autumn and winter. Datasets varying depending on season selection will be annotated accordingly. If not noted otherwise, seasons are defined as meteorological seasons of the Southern Hemisphere. Midnight of the first day of the selected season always marks $\tau = 1$ and $t = 0$ h of a run.

Weather data is used to determine the power output of photovoltaic (PV) installations, *vide infra*. Specifically, solar irradiance ϕ_τ and surface air temperature T_τ are utilised

Algorithm 1 High-level notation of proposed agent based model

```
// Initialisation: Environment
Generate weather, areas, roads and companies
// Initialisation: Agents
Generate agents (EV and Residence)
Generate agents' schedules
// Simulation
for int τ = 1; τ ≤ τ_max; τ++ do
    Update Environment
    for int i = 0; i ≤ n; i++ do
        Update residence
        Update EVs
    end for
end for
// Finalisation
Evaluate simulation results
```

which do depend on the selected season. For each run, time series for ϕ_τ and T_τ are composed of historic data. The values of each time series are drawn at random from all entries in the historic dataset, which match both date (neglecting the year) and time for the corresponding τ.

2.1.2 Map

Our proposed model features EV agents moving across a map consisting of areas and roads. Drafting a graph theoretic analogy, areas can be considered vertices while roads can be considered edges. These elements form the basis of the road network which agents use to commute between home and work.

Areas are geographic locations where agents live and work. Each area can be identified either by its code, Name or GPS centre coordinates. The code and name are as defined by the Australian Bureau of Statistics's Statistical Area Level 3. Areas are characterised by a number of parameters which define housing conditions for its residence. Each agent lives in its own residential dwellings (for brevity, the qualifying "residential" is dropped), also referred to as the agent's home. These dwellings are either of type "apartment", "house without PV" or "house with PV", with n_a, n_{wo} and n_w denoting the amount of dwellings of each respective type in an area. PV capacity P_{PV} indicates the capacity of the PV assets installed on each dwelling of type "House with PV" in this area. For each area there is also a statistic provided, breaking down household sizes. An overview of most area parameters is given in Table 1 in the appendix.

Areas are connected by bidirectional roads where the connections are determined by the areas' geographic features as described in the appendix. Figure 1 shows a stylised map depicting all considered areas and roads. Agents travel on roads at velocity $v_a = 63$ km/h, which is the rounded down "average speed across each road segment in [Melbourne's] arterial road network" (Australian Automobile Association, 2019). The length $l_{\alpha,\beta}$ of a road connecting area α and β is determined using the areas' centre coordinates and the Haversine formula.

Furthermore, each area hosts public charging infrastructure, where EVs can be charge at a maximum charge rate $cr^p = 50$ kW at a price of $p^p = 0.52$ \$/kWh. While this specific value is taken from Tesla's superchargers, it appears representative for Level 3 charging in Australia (JOLT Charge Pty Ltd., 2021; Parkinson, 2020).

2.1.3 Companies

Each area hosts one company employing all agents working in this area. Each company can be equipped with charging stations for its employees. The number of chargers installed at each individual company is set to be the rounded up quotient of the number of employees divided by a preset employee-per-charger ratio r_{epc}. Chargers installed on company sites are AC-chargers with maximum charge rate $cr^w = 25$ kW. Employees pay p^w

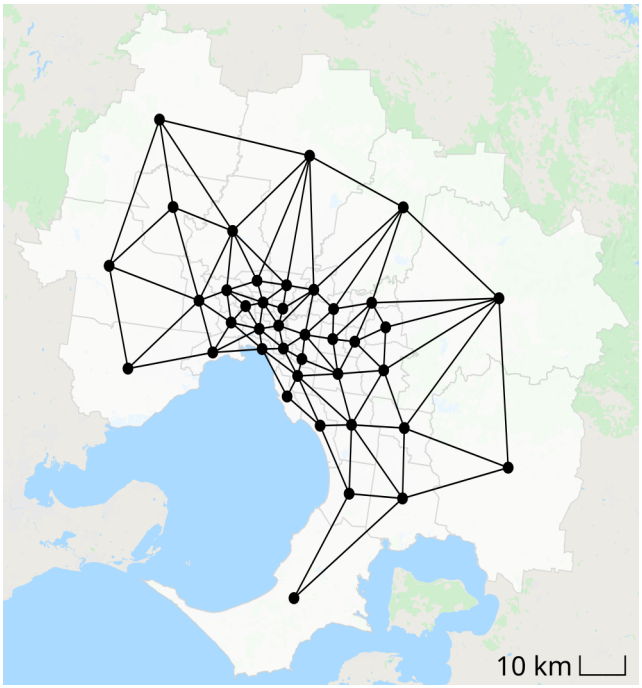

Figure 1: Map of Melbourne. White patches with grey borders show selected areas following Statistical Area Level 3 definition (ABS Geospatial Solutions, 2020). Black circles represent area centre coordinates. Black lines represent available roads to travel between areas. Underlying map images collected from Snazzy Maps (Adam Krogh, 2021). Scale derived from Google Maps (Google Australia Pty Ltd, 2021).

for utilising these chargers.

2.2 Initialisation of Agents

Once the environment has been initialised, a total of n agents is generated. Agents consist of two components: a residence and an EV. The residence refers to the dwelling the agent inhabits. The EV component represents the vehicle the agent uses to commute between its residence and the company employing the agent. All agents are heterogeneous in nature where each agent possess unique attributes and work schedules.

2.2.1 Residences

For each created agent, a residence is created and assigned to this agent and this agent only. Each residence is also assigned to an area through a surjective mapping. Which

area the residence is assigned to, is drawn at random from a list of all areas weighted by the sum of their respective m-person-households. Subsequently, the dwelling type and household size is determined at random using weighted lists based on the assigned area's statistics.

Given the residence's area (home area), the area hosting the company employing the agent (work area) is drawn at random from a weighted list of all areas. The weights represent the amount of people from the home area employed in the work area. If the agent's home area is its work area, the commute distance is drawn at random from a weighted list of people's commute distances when living and working in this area. The one way distance between home and work area is denoted l^{ow}. Anticipating Section 2.3.2, the energy needed to drive an EV for l^{ow} depends on the car model and is denoted q^{ow}.

The residences' electricity consumption excluding EV charging is denoted d_τ. To account for temporal difference in consumption a baseline-normal-distribution is used defined by mean $\mu^d_{\tau_{week}}$ and standard deviation $\sigma^d_{\tau_{week}}$ with $t_{week} = \tau_{week} \cdot \Delta t = (\tau \cdot \Delta t)\%(7 \cdot 24 \text{ h})$. Consumption deviation δd, that is a deviation from the baseline distribution, depends on the area, season and household size. More details on dwelling consumption are given in Section 2.3.1

Each dwelling of type "house with PV" or "house without PV" has an AC-charger installed with a maximum charge rate $cr^r = 2.4$ kW. Dwellings of type "apartment" do not provide a charger. All dwellings purchase electricity at a rate $p^g = 0.27$ \$/kWh which resembles the rounded average Australian residential flatrate tariff (Mountain, 2017). Dwellings of type "house with PV" do have rooftop PV installations with capacity P_{PV}. Electricity can be fed into the grid at a feed-in-tariff rate $p^f = 0.07$ \$/kWh, representing the rounded current feed-in tariff in Australia (Essential Services Commission, 2021). Dwellings of other types do not have PV assets installed, that is $P_{PV} = 0$ m^2. The unit m^2 does not represent the surface area of the PV panels but considers multiple factors impacting the asset's performance.

2.2.2 Electric vehicle

This simulation implements various car models. Each car model is characterised by its battery capacity b, AC charger capacity cr^{AC}, DC charger capacity cr^{DC} and consumption rate[1] c. The EV's state-of-charge soc is initialised to be $soc = 20\% = \frac{1}{5}b$, with the relative quantity referring to the ratio between stored electric energy and b. A list of all implemented car models can be found in Table 3 in the Appendix.

During the simulation's initialisation, each agent is assigned a car model at random. However, the agent is constraint to only choose from car models which ensure: A) $2q^{ow} \leq \frac{3}{5}b$ and B) $q^{ow} \leq cr^{w} \cdot 6$ h.

Charge rates have been implemented as constant functions over time. This simplification is justified as this simulation sees the majority of EV's satisfy $20\% \leq soc \leq 80\%$ at all times. Also for simplicity, this model neglects charging losses.

2.2.3 Schedules

Agents are assigned one of three activities: being at home, being at work or commuting. An individual schedule determines at what time an agent performs which activity and are repeated every week. The schedules are based on statistics describing the amount of hours Australians work per week and at what point in time Australians are working. The detailed scheduling methodology can be found in the appendix.

It is noted that this model does not consider any travel apart from the commute between work and home. This modelling decision was made, as to the best of our knowledge there exist no driving diaries or statistics measuring when agents are travelling for other reasons than work in the selected Melbourne area. An implantation of non-work related driving would therefore be as speculative as neglecting it. While this simplification may appear drastic, it reflects the most common behaviour in daily human mobility patterns,

[1]Initially, the approach described in (Chaudhari et al., 2019) was implemented to calculate EV consumption. However, with minute-sized time steps, parameters like acceleration and road gradients were monitored to coarse. Omitting these parameters from the instantaneous consumption calculation led to consumption rates smaller than the manufacturer's consumption claims. Thus, this model will use the consumption rates provided by manufacturers.

vide supra.

2.3 Simulation

Once the model is initialised, the simulation enters an interactive process in which the model's dynamics are calculated in discrete time steps. As indicated in Algorithm 1, each τ can be broken down into three substeps. First, the environmental parameters are updated. However, as this only encompasses ticking forward the in-simulation-time and with that the time series for ϕ_τ and T_τ, this step is not described in an individual section. Second, the impact of the environmental changes on the individual residences is evaluated. Once this impact has been calculated for all residences, the last substep sees the calculation of EV dynamics. Here both EV movement and EV charging are computed for an agent before continuing with the next agent. The order in which both residences and EVs are calculated is drawn at random for each τ individually.

Given τ_{max} and Δt, each run covers two week. The first simulated week is considered a pre-heat phase, with results of this phase not being recorded. Only the second week's 2016 time steps are recorded and presented in Section 3.

2.3.1 Residence dynamics

Determining d_τ, the agent draws $\tilde{d}$ at random from the baseline-normal-distribution with means $\mu^d_{\tau_{week}}$ and standard deviation $\sigma^d_{\tau_{week}}$. If $\tilde{d} < 0$ kW, it is re-drawn. Then, $d_\tau = \tilde{d} \cdot \delta d$. For a given ϕ_τ and T_τ the PV generation rate of each dwelling is:

$$P_\tau = P_{PV}\phi_\tau(1 - \frac{T_\tau}{200\text{ K}}) \tag{1}$$

2.3.2 Electric vehicle planning and movement

In a given time step $\tilde{\tau}$, each EV goes through three phases: Planning for the current time step, if necessary move to a new location and charge if desired. These phases and high-level logic steps are depicted in Figure 2.

The planning phase encompasses most decisions, which characterise the behaviour of

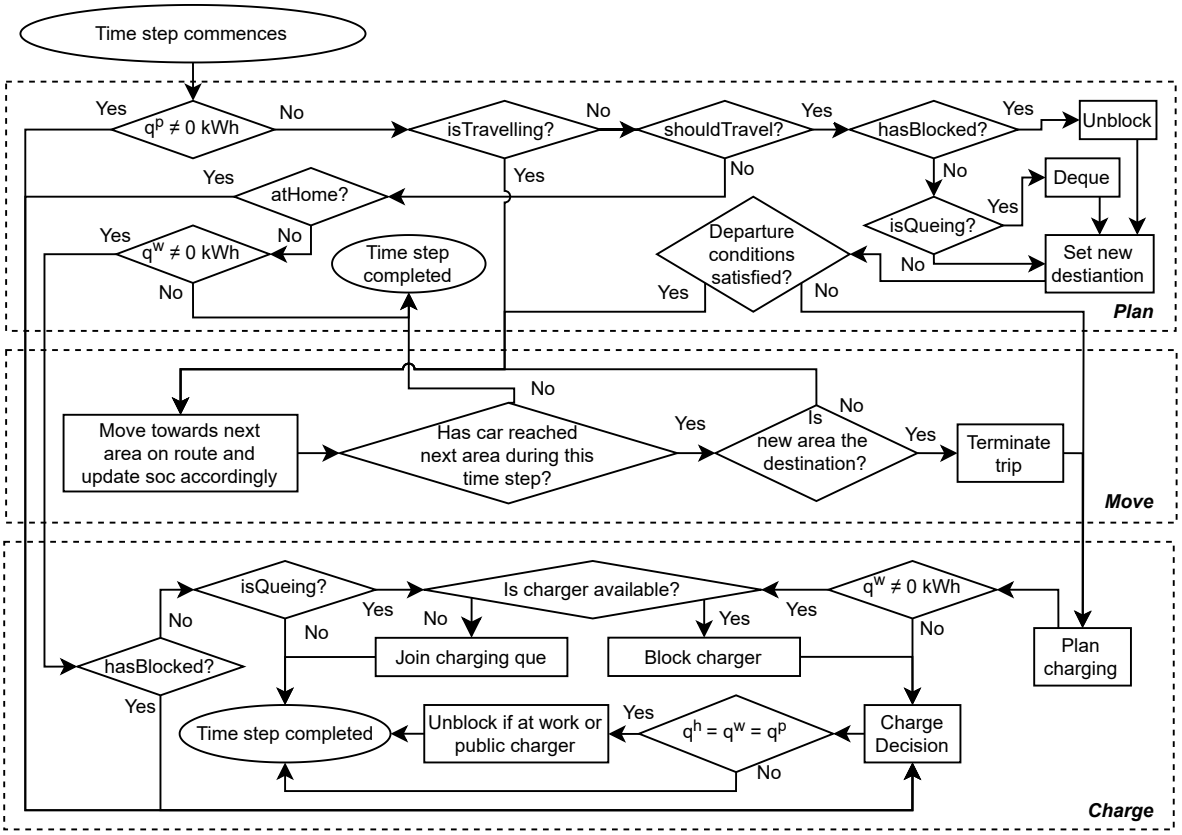

Figure 2: Overview EV-Agent logic showing three phases: Plan, Move and Charge.

the EV in the current and coming time steps, excluding the decision of how much the EV should charge. The most prominent decision taken here is if the EV should commence a new journey. As prerequisites to decide when to depart on a new journey, the agent is aware of the amount of time steps it needs to reach its next destination τ_c, which due to the commute being limited to one route can be considered a constant. Also, the agent attempts to arrive $\tau_r \cdot \Delta t = 10$ min early at work.

The agent should commence its commute from home to work if it is not at work, is not travelling and $\tilde{\tau} \geq \tau_S - \tau_c - \tau_r$ with τ_S being the time step the agent's next shifts starts. Similarly, the agent should commence its commute from work to home if the agent is not at home, is not travelling and $\tilde{\tau} \geq \tau_E$ with τ_E denoting the time step the agent's current shift ends. In both cases, set shouldTravel = true, unblock any blocked charger and remove agent from any charging queue, *vide infra*. Otherwise, set shouldTravel = false.

When receiving the trigger shouldTravel = true, the agent checks the departure con-

dition

$$soc \geq q^{ow} + q^{em} = q^{ow} + \max\left(\tfrac{1}{5}b, c \cdot l^{em}\right), \tag{2}$$

with q^{em} being the agent's reserve and $l^{em} = 50$ km being the reserve range. If the departure condition is not satisfied, the agent starts to plan its next charging stop, compare Section 2.3.3. Otherwise, the agent sets isTravelling = true and calculates the shortest route to its next destination, resulting in the aforementioned length of the upcoming route l^{ow}.

Given v_a, travelling agents cover up to 5.25 km per time step. Once the agent arrives at its destination, the agent sets isTravelling = false and calculates its charging needs. The latter is explained in the following section.

2.3.3 Electric vehicle charging

In this model, EV charging comprises three components: charge quantity determination, charger acquisition and the charging process itself. In this order, each component depends on the preceding component. Charge quantity determination is triggered whenever the agent either terminates a journey or is about to commence a new journey but could not satisfy the departure condition.

Charge quantity determination: The charge quantity determines how much the agent should charge in the current and following time steps from a specified source. In this work, three different scenarios are discussed to determine this quantity:

1. No Work (nw): No chargers are available at work. Agents aim to charge their car to $soc = 80\%$.

2. Basic Charging (bsc): Chargers are available at work. Agents will perform a basic price comparison and prefer to charge their EV to $soc = 80\%$ where price is cheaper.

3. Advanced Charging (adv): Chargers are available at work. Agents will perform a price comparison including the consideration of the expected future yield of their

rooftop PV assets. Optimising *soc* for charging cost, q^{em} is keep as reserve at all times but not aiming for $soc = 80\%$.

The charge quantity depends on the agent's location, dwelling type and timing. The source to charge from is indicated by what variable the quantity is assigned to. If the determined quantity is to be charged at home, work or at a public charger, the quantity is assigned to q^h, q^w or q^p, respectively. Whenever one of these variables is assigned to, the other two variables are set to zero. For the prices, it is assumed that $p^f < p^p$ and $p^f < p^g$ and $p^w < p^p$.

Under all three scenarios, if the agent is about to commence a journey and the departure condition is unsatisfied, the agent uses faster public charging to acquire the missing charge needed to satisfy the departure condition. That is:

$$q^p = [q^{ow} + q^{em}]^+, \tag{3}$$

with $[\circ]^+ = \max(\circ - soc, 0)$, where $\circ$ reflects the desired *soc* the car shall charge to.

Under scenario nw, upon arrival at home, assign:

$$q^h = [\tfrac{4}{5}b]^+, \text{ if } p^g \leq p^p \tag{4}$$

$$q^p = [\tfrac{4}{5}b]^+, \text{ if } p^p < p^g \tag{5}$$

Under scenario nw, upon arrival at work, assign:

$$q^p = [q^{ow} + q^{em}]^+, \text{ if } p^g \leq p^p \tag{6}$$

$$q^p = [\tfrac{4}{5}b]^+, \text{ if } p^p < p^g \tag{7}$$

Under scenario bsc, upon arrival at home, assign:

$$q^p = [q^{ow} + q^{em}]^+, \text{ if } p^p < p^g \tag{8}$$

$$q^h = [q^{ow} + q^{em}]^+, \text{ if } p^w < p^g \leq p^p \tag{9}$$

$$q^h = [\tfrac{4}{5}b]^+, \text{ if } p^g \leq p^w \tag{10}$$

Under scenario bsc, upon arrival at work, assign:

$$q^w = [q^{ow} + q^{em}]^+, \text{ if } p^g < p^w \tag{11}$$

$$q^w = [\tfrac{4}{5}b]^+, \text{ if } p^w \leq p^g \tag{12}$$

Under scenario adv, upon arrival at home, assign:

$$q^h = [2q^{ow} + q^{em}]^+, \text{ if } p^g \leq p^w \tag{13}$$

$$q^h = [q^{ow} + q^{em}]^+, \text{ if } p^w < p^g \leq p^p \tag{14}$$

$$q^p = [q^{ow} + q^{em}]^+, \text{ if } p^p < p^g \tag{15}$$

Under scenario adv, upon arrival at work, assign:

$$q^w = [2q^{ow} + q^{em}]^+, \text{ if } p^w \leq p^f \text{ or } p^p < p^g \tag{16}$$

$$q^w = [2q^{ow} + q^{em} - [R]^{\pm}]^+, \text{ if } p^f < p^w < p^g \leq p^p \tag{17}$$

$$q^w = [q^{ow} + q^{em}]^+, \text{ if } p^g \leq p^w \tag{18}$$

with $[\circ]^{\pm} = \min(\max(\circ, 0), q^{ow})$ and

$$R = \mu + \sqrt{2}\sigma \operatorname{erf}^{-1}\left((1-2\alpha)\left(1 - \frac{p^g - p^f}{p^g - p^w}\right) - 1\right), \tag{19}$$

where $\alpha = 0.9$ is the agent's confidence which is defined to be constant in this work. The variables μ and σ are the mean and standard deviation of the forecast-normal-distribution. This distribution is a measure for the amount of electrical energy generated

by the agent's PV assets which exceeds the residence demand as defined as d. Note the missing subscript for μ and σ. This is because the forecast-normal distribution describes the energy generated from the time step after the agent reaches its residence τ_R until the time step the agent departs again from its residence τ_D, that is

$$\mu = \mu^{PV}(\tau_R, \tau_D) - \sum_{\tau=\tau_R}^{\tau_D-1} \mu_\tau^d \tag{20}$$

$$\sigma = \sqrt{(\sigma^{PV}(\tau_R, \tau_D))^2 - \sum_{\tau=\tau_R}^{\tau_D-1} (\sigma_\tau^d)^2}, \tag{21}$$

where $\mu^{PV}(\tau_R, \tau_D)$ and $\sigma^{PV}(\tau_R, \tau_D)$ parameterise a normal distribution describing the amount of electric energy generated by the agent's PV assets from τ_R to τ_D. Both functions are derived from historic data as shown in the appendix.

While most of the equations above describe EVs charging either the amount needed to complete the next trip (see Equations (3, 6, 8, 9, 11, 14, 15, 18)), the next trip including return (see Equations (13, 16)) or charge up to $soc = 80\%$ (see Equations (4, 5, 7, 10, 12)), Equation (17) differs by including a risk term which is described in Equation (19). The derivation of the risk term can be found in the appendix. Based on the Conditional Value at Risk measure, R allows each agent to estimate the generation of its rooftop PV asset during the agent's next stay at home. The agent can then refrain from charging as much at work and instead rely on its PV asset. Exemplarily, the quantity q^{hb} an agent in a given state under scenario adv, ideally foregoes at work is shown in Figure 3b). For the same state and scenario, Figure 3a) shows the ideal quantity charged at work.

Some parameters are adjusted for agents of a particular dwelling type. For agents with dwellings of type "Apartment" set $p^p < p^g$. For agents with dwellings of type "House without PV" and "Apartment" set $\mu = \sigma = 0$ kWh. These changes will prevent agents from using assets which they do not have access to.

Once the charge quantity is determined, the agent checks if this quantity needs to be increased to ensure the lowest possible cost. This is the case when an upcoming stay near the cheapest charging source is so short that a more expensive charging source will have

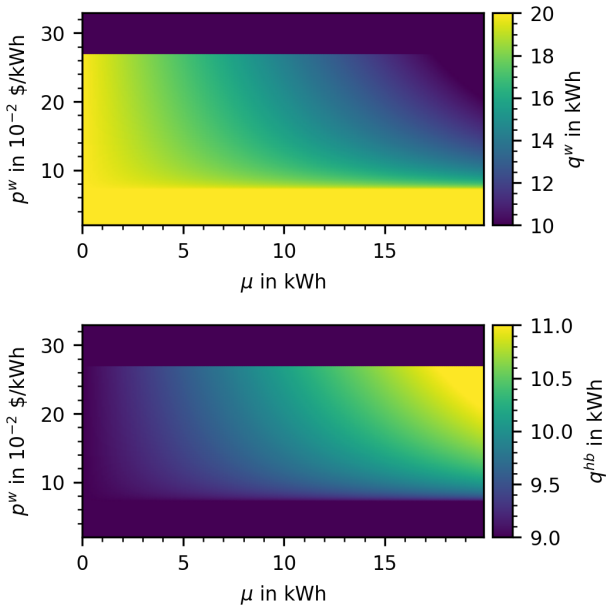

Figure 3: Figures show the ideal charging at work under scenario adv. Assumes approximated ratio $\sigma = \mu/3$. Parameters used: $q^{ow} = 10$ kWh, $soc = 5$ kWh, $q^{em} = 5$ kWh.

to be used in the future. Then, while considering its batteries constraints and considering all stays between the current time step and the stays leading to a violation of departure condition, the agent increases its current charge quantity as necessary.

Charger Aquisition: Public chargers are always available to agents (consider an infinite number of public chargers) and each agent with a dwelling of type “House without PV" or “House with PV" has its own charger at its residence. Thus, if an agent decides to use public charging or to charge at home they can acquire a charger without restriction. However, chargers at work might be limited. Thus, not each agent wanting to charge at work at time step τ might be able to do so. To manage the existing chargers, agents have to block available chargers they intend to use, that is, a charger is assigned to an agent. This procedure looks as follows:

An agent arriving at work, determining $q^w \neq 0$ kWh and attempts to block a charger. In case, a charger is available, the free charger is assigned to the agent until the agent leaves work unblocking the charger. In case no charger is available, the agent queues for a charger. Once a different agent unblocks a charger at the same company, the agent who is queuing for the longest time can dequeue and block the freed up charger.

Charging process: Once an agent has acquired a charger, its EV can charge with a charge rate depending on the type of charger used: For home chargers $cr = \min(cr^{AC}, cr^{h})$, for work chargers $cr = \min(cr^{AC}, cr^{w})$ and for public chargers $cr = \min(cr^{DC}, cr^{p})$.

Agents that have acquired work or public chargers will start charging immediately. Each time step, these agents charge $q^c = \max(\Delta t \cdot cr, q^w)$ or $q^c = \max(\Delta t \cdot cr, q^p)$, respectively. At the end of each time step, q^c is subtracted from then corresponding charge quantity.

Agents arriving at their residence of dwelling type "Houses with PV" aim to maximise their rooftop PV utilisation. As a consequence, in case $p^f \leq p^w$, the agent delays charging until time step $\tau = \tau_S - \tau_c - \tau_r - [q^h \cdot \Delta t / cr]^*$ with $[\circ]^*$ rounding $\circ$ up to the next integer. During the entirety of the agent's stay at home, the agent charges the excess energy generated by its rooftop PV asset which is not consumed by its residence respecting its chargers' limits. As before, all charged electric energy is subtracted from the charge quantity. Agents arriving at their residence of dwelling type "Houses without PV" behave similar but do not charge from PV.

Charging ends for all agents once the charge quantity has been reduced to zero. As an exception under scenario adv, agents charging their rooftop PV's excess energy will only stop charging once $soc = b$. Upon departure, agents charging or queuing at work will unblock their acquired chargers or leave the queue, respectively.

2.4 Finalisation

After the last time step is calculated, a number of quantities are provided to analyse the simulation, which this section explains. Each quantity, say X, can be filtered using three subscripts, that is $X_{\dagger,\circ,*,}$. The subscript $\dagger$ specifies the employed scenario (nw, bsc or adv), $\circ$ allows considering only the contribution of one source (public charging, work place charging, charging at home from grid or charging PV excess energy) to X and $*$ allows to only consider agents of a certain dwelling type. In the figures provided in the next chapters, we will use the symbols $\dagger, \circ$ and $*$ in case the plot's legend or caption explains what to insert for each symbol. We will drop $\circ$ or $*$ if all sources or all dwelling

types are aggregated, respectively.

The quantities returned are: The average price per kilometre $C^{avg}_{\dagger,\circ,*}$ paid by each agent when commuting. The charge rate $cr^{ts}_{\dagger,\circ,*,\diamond}$ summing the rate of charge each charger provides in the current time step, with optional $\diamond$-subscript allowing to specify an area where the charge is withdrawn. The charge delivered $cd^{tot}_{\dagger,\circ,*,\diamond}$ by all chargers over the simulation's course, with optional $\diamond$-subscript as for $cr^{ts}_{\dagger,\circ,*,\diamond}$. The average charger utilisation $U^{avg}_{\dagger,\circ,*}$ is the ratio between all work place chargers blocked and those unblocked during a time step averaged overall time steps. And lastly, the revenue $R^{tot}_{\dagger,\circ,*}$ each employer generates by letting employees charge at their company over the simulation's course.

Each scenario was simulated for each season. The results presented in the next section are averaged over all seasons. Time shown in the results is offset by one week to compensate for the first dropped week. To reduce computational burden, only a fraction of the total $\hat{n} = 1.2 \cdot 10^6$ people living in the selected area commuting by car as drivers have been simulated. Results have then scaled to $\hat{n}$ as indicated for each depicted result.

3 Results

The simulation results are organised according to different stakeholder groups and their relevant interests, this consist of consumers, companies and grid operators. The consumer group focuses on overall charging cost whilst the interest of companies are biased towards factors that affect revenue. The results also provide grid operators with some indication of how charging load will shift if workplace charging becomes prevalent, in both the temporal and spatial domains.

3.1 Consumers

Figure 4 depicts the changes in average cost of charging when both workplace charger availability and price are varied. A significant transition occurs at the flat rate tariff $p^g = 0.27$ \$/ kWh for home charging. This can be attributed to the majority of agents having access to home chargers where it becomes no longer economically justifiable to

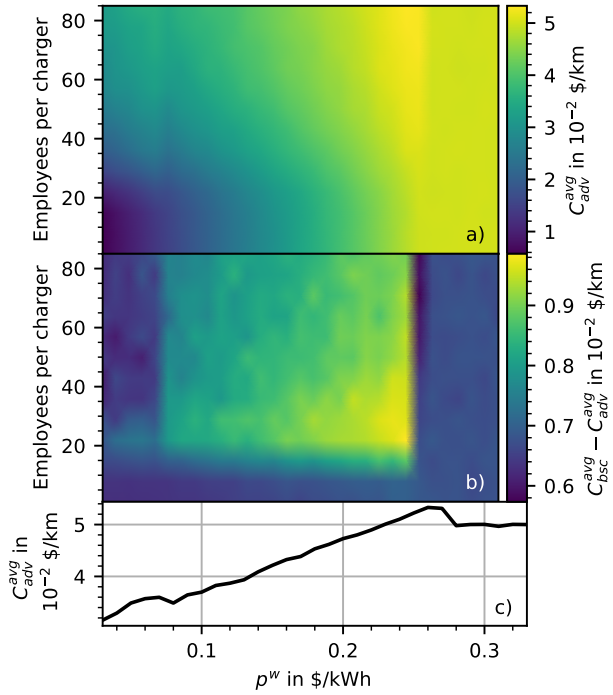

Figure 4: Average cost of travel per km depending on charger availability and workplace charging price p^w. Fig c) isolates the case for 85 employees per charger. Computed $n = 2.4 \cdot 10^3$, no scaling necessary.

charge at work when the cost of workplace charging is greater than home charging.

Figure 4a) represents how the average cost of charging varies when the proposed charging strategy under scenario adv is utilised. The cost of charging peaks when the price of workplace charging is set to just below p^g in conjunction with a high demand for workplace chargers. As workplace charging is cheaper than charging at home, this is the preferred source of charging. However, as all agents are employing the same strategy, there is a common expectation that a charger will be available upon arrival at work. This high demand of cheaper charging results in limited availability of workplace chargers which subjects individuals to uncertainty of securing a charger. Subsequently, a greater reliance on the public DC charging network occurs to meet the energy requirements for the proportion of the population unable to secure a workplace charger and unable to return to their residences.

The difference in average charging cost between scenario adv and bsc is highlighted in Figure 4b). The magnitude can be interpreted as the extent of the advanced charging

strategy's effectiveness at reducing charging costs compared to the basic charging strategy. The inclusion of a parameter sweep for workplace charger availability results in a saturation point occurring around 15 to 20 employees per charger. This represents the number of employees who can be reliably served by a single charger before the effects of uncertainty regarding charger availability occurs; subjecting individuals to the possibility of charging from more expensive sources. Evidently, peak difference in average costs between the two charging approaches occurs at this saturation point and when the price of workplace charging is just below the flat rate tariff for home charging. This demonstrates the cost saving potential of withholding charge where individuals are not subjected to unnecessary charging costs associated with workplace charger uncertainty.

The effect of an agent's choice in charging source on workplace charger demand and subsequent exposure to charger availability can be seen in Figure 4c). A decrease in average cost, despite the increase in p^w, can be observed at the values of $p^f = 0.07\$/$ kWh and p^g. This represents a migration in the choice of preferred primary charging source for a proportion of the population resulting in a momentary drop in workplace charger demand. This preference is driven by dwelling type and subsequent access to a home charger where the presence of PV is a determining factor.

Charging cost variations seen in Figure 4b) and c) can be attributed to agents' behaviour as defined by Equation (16-18) where charge is withheld in anticipation for charging at a lower cost. Workplace charging is the preferred source for the entire population if $p^w < p^f$. When the price of workplace charging exceeds the feed-in tariff, the primary source of charging changes for the proportion of the population with access to a home charger and a PV installation. This can be visualised as a branching effect seen in Figure 5a) where average travel cost is no longer entirely dependent on p^w. However, this subset of the population still utilises the workplace as a secondary charging source as it still remains less than p^g. Subsequently, there is a diminished effect of increasing cost of travel for PV owners. However, this plateaus after workplace charging exceeds p^g. The majority of the population switches to home charging as the preferred primary charging source at this price point where another branching effect is evident. Similarly, the cost

of travel for these individuals settles where there is minimal dependency on p^w. Apartment dwellers and other individuals without access to a home charger will still rely on workplace charging as the primary source, where the average travel cost is dependent on p^w.

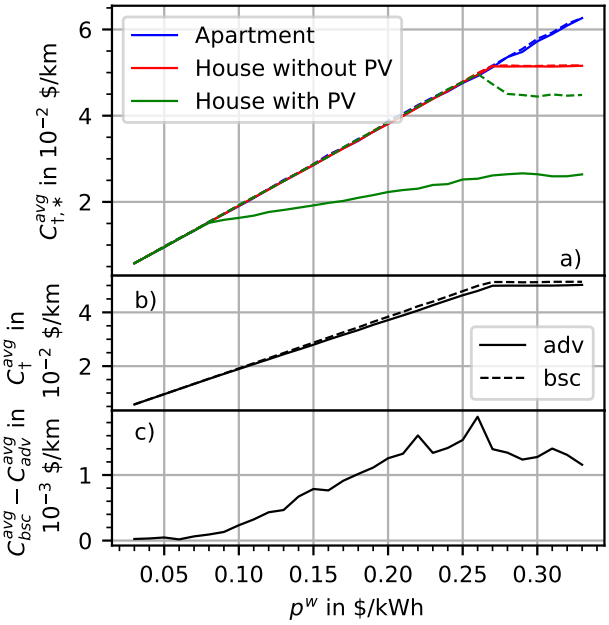

Figure 5: Overall average charging cost for each dwelling type. Computed $n = 6.0 \cdot 10^3$, scaled to $\hat{n}$. $r_{epc} = 1$.

The aggregate effect of employing the advanced charging strategy over the basic charging approach can be visualised in Figure 5b). Evidently, the cost saving potential of 2% on average is low when observing across the entire working population as dwellings with PV only constitute for only 12% of the population. Figure 5c) highlights where the peak difference in the two charging approaches occurs, when p^w is just slightly less than p^g. In general, the advanced charging strategy proposed optimises for better utilisation of PV which can be observed in the detailed breakdown of charging by source type across a week as seen in Figure 6. A significant difference in how PV is incorporated into the weekly charging cycle can be observed by comparing the advanced charging approach as seen in Figure 6a) to the basic charging approach represented by Figure 6b). Workplace charging represents the primary source of charging during weekdays by an order of magnitude compared to the next preferred source of charging for the advanced charging

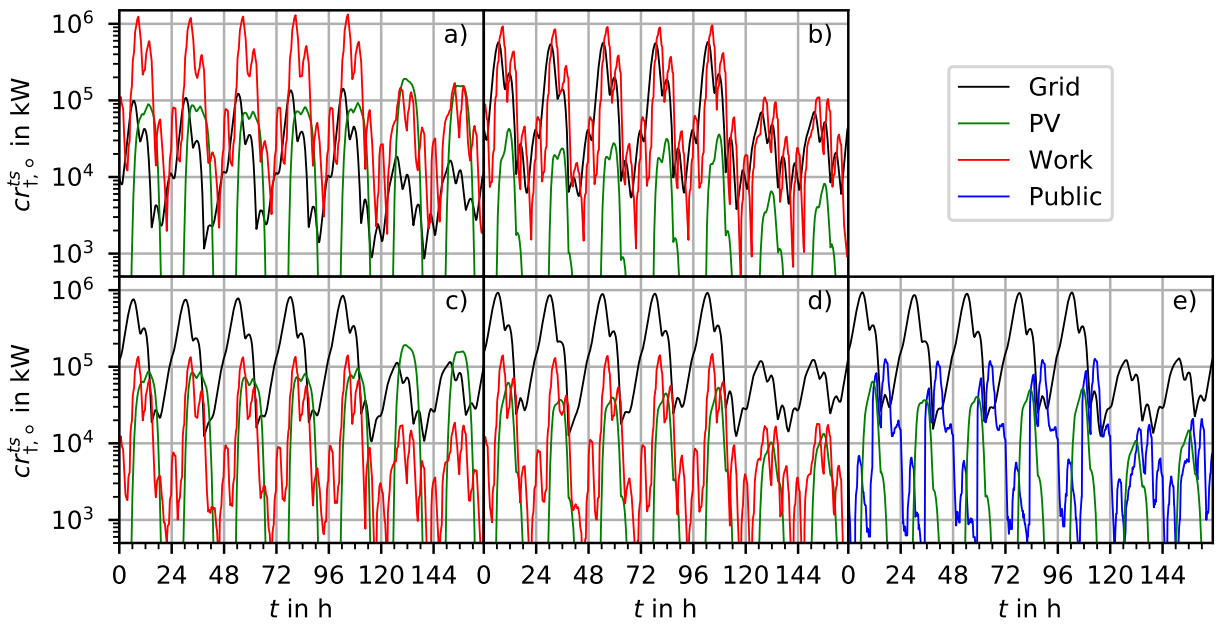

Figure 6: Charge delivered by source. Fig a) Advanced, $p^w = \$0.27$, $r_{epc} = 1$. Fig b) Basic $p^w = \$0.27$, $r_{epc} = 1$. Fig c) Advanced, $p^w = \$0.28$, $r_{epc} = 1$. Fig d) Basic $p^w = \$0.28$, $r_{epc} = 1$. Fig e) No workplace chargers. Moving average over 1 hour. Computed $n = 1.2 \cdot 10^4$, scaled to $\hat{n}$.

strategy. Moreover, reliance on charging from the grid is reduced on the weekends where a greater increase in PV charging can be observed with the difference being an order of magnitude. Conversely, the basic charging approach visualised by Figure 6b) showcases an equal reliance on both workplace and home charging from the grid across the entire week. Most noticeably, PV is utilised as the tertiary source of charging when there is no provision for withholding charge.

A similar distribution of source types in Figure 6a) is reflected in Figure 6c) which represents the advanced charging strategy when $p^w > p^g$. The only difference is the substitution of primary charging source from workplace to home charging. The same analysis is applied to the basic charging approach where $p^w > p^g$ where reliance on workplace charging decreases by an order of magnitude as seen in Figure 6d). Whilst possessing a similar distribution profile in source type to the advanced charging strategy at this higher price point, there is significantly less charging from PV on the weekend. This highlights the main difference between the charging approaches where provisions for weekend charging from PV can occur when the advanced charging strategy is utilised.

A comparable make-up of source type can be observed in Figure 6e) which represents a scenario where there are no workplace chargers where public charging replaces the same demand that workplace charging satisfies in Figure 6d). This scenario is indicative of a small market share of EVs where the economies of scale for the installation of workplace chargers have not yet fully developed to be financially viable on a large scale.

3.2 Companies

Figure 7 showcases the effect increased access to PV has on preferred charging sources, expected revenue of workplace chargers and utilisation rates. This assumes a scenario where an employer provides each employee with a dedicated charger, representing maximum reliance on workplace charging where possible. The accumulated charge delivered by source type over a time period of a week is shown in Figure 7a) and b); the former representing a scenario based on current dwelling statistics whilst the latter showcases a scenario where all dwelling types have access to rooftop PV and home charging. As the uptake of rooftop PV increases, the realistic outcome will most likely be situated somewhere between these two scenarios. The composition of charging sources in Figure 7a) represents the aggregated distributions presented in Figure 6 where p^w is varied. As expected, workplace charging remains the preferred source of charging when $p^w < p^f$. However, this changes when $p^f < p^w < p^g$ where charging from PV becomes the primary source of charge depending on the penetration level of rooftop PV as seen in Figure 7b). Consequently, the decrease in reliance on workplace charging is reflected in the revenue and utilisation rates, as seen in Figure 7c), d), e) and f) respectively. This highlights how the uptake rate of rooftop PV can have an impact on the prospect of long-term financial viability regarding recuperation potential of workplace chargers. Evidently, the significant decrease in revenue seen in Figure 7c) and d) is inherently related to the utilisation rate of workplace chargers represented by Figure 7e) and f).

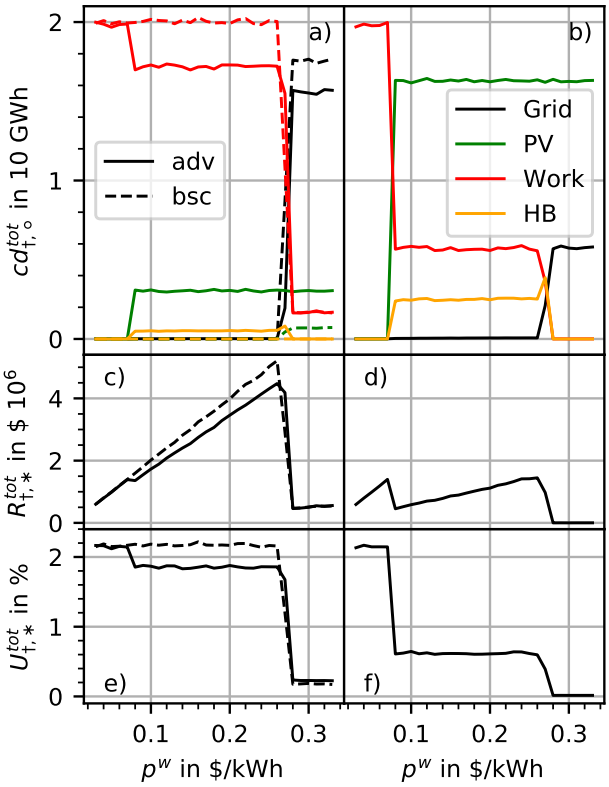

Figure 7: Simulation of different scenarios consisting of varying dwelling types and PV penetration levels. Fig. a) + c) + e) represent dwelling types as per census statistic. Fig. b) + d) + f) All dwellings are houses with PV. Fig. a) + b) Charge delivered by source. Fig. c) + d) Accumulated revenue of all companies. Fig. e) + f) Average charger utilisation between all companies. Simulated over one week, legend in Fig a) applies to all figures. Computed $n = 2.4 \cdot 10^3$, scaled to $\hat{n}$. $r_{epc} = 1$.

3.3 Grid planners and operators

The widespread adoption of EVs and subsequent reliance on workplace charging will result in load shifts across the electrical network. Grid operators will require some indication on where addition infrastructure planning is needed for future demand depending on the preferred source of charging. Figure 8 represents the use of the advanced charging strategy compared to a scenario where no workplace charging is available, where the difference is analysed in both the temporal and spatial domain. A change in preferred source of charging can be inferred from the workplace charging peaks on the weekdays in Figure 8a) which coincides with the negative demand of home charging. Charging demand on the weekend remains relatively unchanged except for a slight increase in charging from PV.

Figure 8b) represents a high level overview of how charging demand will be affected in the context of metropolitan Melbourne. This provides some indication on how the load from charging EVs might shift to different regions when workplace charging becomes a common occurrence. The shift in demand to workplace charging in the red regions coincide with high-density commercial and residential areas such as the central business district (CBD). Furthermore, the blue regions indicate a greater reliance on home charging which is indicative of the outer suburbs consisting of mainly low-density housing. In this case, workplace charging has been priced such that it is the preferred source of charging. However, in specific scenarios outlined in Section 3.1 and 3.2, the distribution will reflect a greater demand for home charging in the outer regions than workplace charging in the CBD.

Figure 8c) represents the charge quantity difference across the two scenarios, comparing the advanced charging strategy to a scenario where no workplace charging is available. The aggregated differences across the regions is shown in addition to the areas which exhibit the greatest differences, where red represents the CBD and blue signifies typical suburbia. Moreover, the typical weekly load profile of the Victorian section of the National Energy Market is presented to highlight how workplace charging impacts peak demand. The expected increase in load from home charging during the evening peak is not observable in the presence of widespread workplace charging. However, the charging behaviour that emerges from employing the advanced charging strategy results in peak charging demand coinciding with the initial morning peak instead. This is due to agents charging upon arriving at work. Similarly, an alignment of the load curves' early morning valley with low demand under the advanced charging strategy can be observed. Another notable feature is the weekend charging pattern where there is a preference for charging from home and PV.

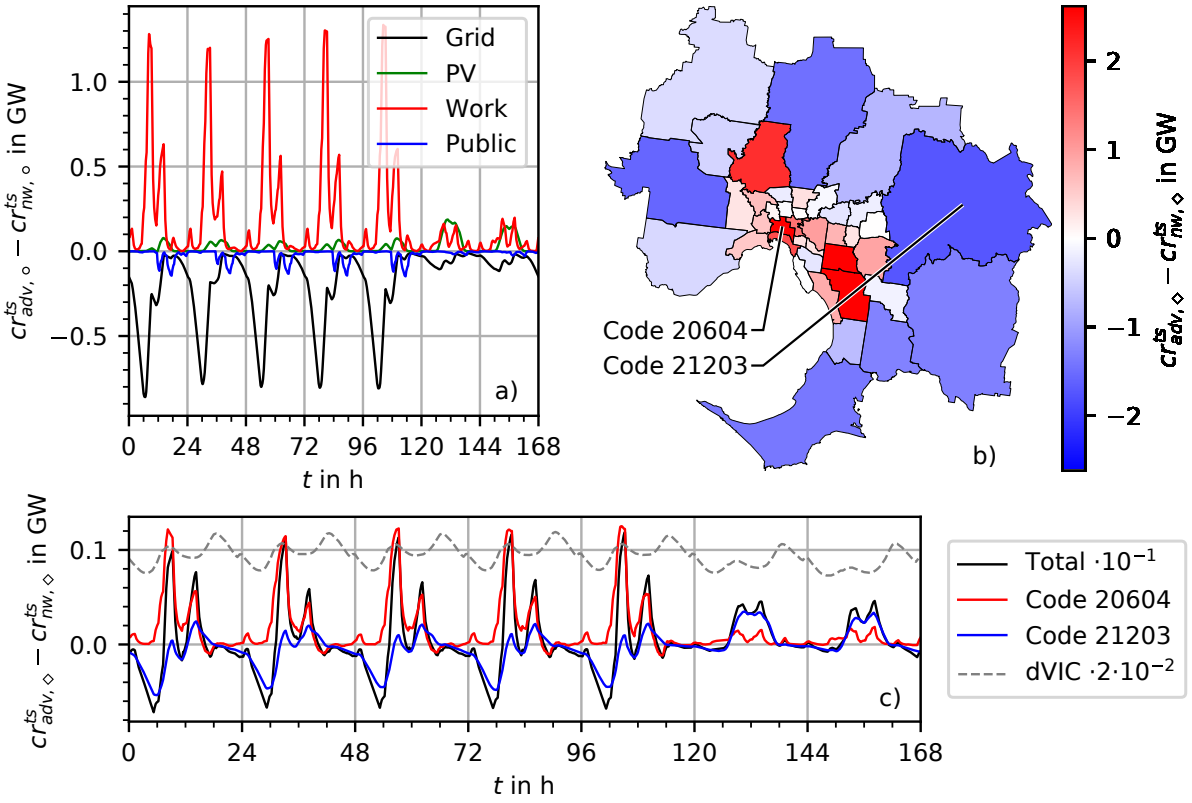

Figure 8: Shift in charging load in the presence of workplace charging. Fig a) Temporal shift of EV charging load between charging sources. Fig b) Spatial shift of total quantity charged between all considered SA3 areas. Fig c) Temporal shift of charge rate for accumulated SA3 areas compared to the average weekly load in the Victorian region of the National Electricity Market (dVIC) in 2020. Computed $n = 1.2 \cdot 10^4$, scaled to $\hat{n}$. For adv scenario: $r_{epc} = 1$.

4 Discussion

The findings from modelling the intricacies of EV charging considering the wider charging infrastructure has formed the basis of this economic framework which highlights various factors that affect the financial viability of workplace charging. The implications relating to the cost variations introduced by the risk aspect associated with PV is twofold. As a micro level parameter, the PV forecast serves as a cost minimisation mechanism for the individual EV user. The cost saving potential is unique to each agent where they are limited by the size of their PV installation and maximum charging rate. In this case, the minimum specifications of home charging was implemented to represent a conven-

tional 10 A wall outlet in Australia, where home charging is limited to 2.4 kW. More realistically, EV owners are likely to install dedicated wall chargers where home charging rates can reach up to 7 kW for a single phase setup. Whilst this will increase the reliance on PV as a preferred charging source in some scenarios, the overall increase of PV uptake will have significant implications on a macro level. The long term financial viability of workplace chargers is negatively affected by an increase in residential rooftop PV. As the preference for primary source of charging shifts, companies will be subjected to lower utilisation rates and revenue. Subsequently, diminishing earning potentials for recuperating the initial installation cost in addition to costs associated with maintenance. This highlights the importance of considering external factors when investigating the economics of workplace charging.

The main limitation of the findings presented above is the assumptions used regarding EV travel patterns. Static home to work commutes are used where there are no provisions for addition travel outside this predetermined route. This is due to a lack of data regarding urban mobility focused on personal use of light vehicles. Simulation of this aspect would require synthesis of two variables; the distance and duration of personal travel. These variables affect the cost minimisation potential significantly due to the reliance of the presence of PV where its generation capability is diurnal in nature. The distance an agent travels directly affects the required charge quantity whilst the duration of travel would define the window of access to home charging. As the outcomes indicate the potential for maximising PV self consumption through increased weekend charging for the proportion of the population that do not work during this period, the uncertainties of duration of personal travel would significantly alter the findings of this paper. Thus, the combination of these two unknown variables would sway the outcomes of the model greatly, potentially producing unrealistic results.

The results presented are based on a case study using metropolitan Melbourne. As such, the findings are specific to the layout of this urban environment where high-density residential and commercial areas are centrally located whilst the outer regions consist of low-density zonings. It is important to note that whilst some commutes occur entirely

within a region, the majority of the population commutes to the CBD. Future extensions could include investigating how these findings change when using different urban environments. This would require census statistics and geographic data of the area of interest where the methodology would remain unchanged. The investigation of a more developed and price competitive public charging network would also be an area of interest for future works.

5 Conclusion

A framework exploring the economics of workplace charging and its long term financial viability was proposed. This was achieved using an agent-based approach which modelled the interactions between EVs and a charging infrastructure consisting of home, workplace and public charging. Additionally, a charging strategy was proposed which aimed to minimise charging cost through incorporation of residential PV self-consumption where a risk aspect associated with forecasting was introduced. The findings indicate that preference in primary source of charging changes depending on the price of workplace charging. Companies could develop pricing schemes to target specific proportions of the population based on dwelling types and associated access to charging infrastructure. Conversely, workplaces were also found to be prone to reduced revenue as the penetration level of residential PV increases, resulting in lower utilisation rates of workplace chargers. However, this assumes a scenario where self-consumption of residential PV and charging cost minimisation are primary objectives of EV users. Finally, the simulation results provide an overview of the expected shift in EV load across the network in both the temporal and spatial domains. The overall findings indicate how different stakeholders will be affected in the presence of prevalent workplace charging infrastructure.

Acknowledgement

This project is supported by the Australian Research Council through project no LP180101309. This research is also supported by an Australian Government Research

Training Program (RTP) Scholarship.

Appenidx

A Area and road determination

The definition of areas follows the Australian Bureau of Statistic's Australian Statistical Geography Standard. This work includes all Level 3 areas composing the following Level 4 areas: 206, 207, 208, 209, 210, 211, 212, 213. Centre coordinates are estimated by averaging all border coordinates defining an area as provided in (ABS Geospatial Solutions, 2020). The Australian Bureau of Statistic's TableBuilder (Australian Bureau of Statistics, 2016), is used to extract data for the selected areas from the 2016 census. This data includes the number of: "Flat or apartment in a one or two storey block", "Flat or apartment in a three storey block", "Flat or apartment in a four or more storey block", "Flat or apartment attached to a house", "Semi-detached, row or terrace house, townhouse etc. with two or more storeys", "Semi-detached, row or terrace house, townhouse etc. with one storey" and "Separate house". All dwellings containing the word "apartment" are counted as n_a. All remaining dwellings are considered houses. For houses, ownership is grouped into either being owned as indicated in TableBuilder by being counted as "Owned outright", "Owned with a mortgage" and "Being purchased under a shared equity scheme" or as being rented which are counted by subtracting the number of owned houses from the total number of houses. Multiplying the number of owned houses and PV density as provided by (Australian Photovoltaic Institute, 2021) results in the number of houses with PV installations n_w. Subtracting n_w from the total number of houses returns the number of houses without PV n_{wo}. The number of people living in the selected areas commuting to work by car as drivers are also extracted from the 2016 census.

Household sizes are taken from TableBuilder as well. One-person-household (1PHH) correspond to "One person"-entries, two-person-household (2PHH) to "Two persons",

three-person-household (3PHH) to “Three persons", four-person-household (4PHH) to “Four persons" and five-or-more-person-household (5+PHH) correspond to the sum of the entries for “Five persons" plus “Six persons" plus “Seven persons" plus “Eight or more persons".

The factor P_{PV} is derived by dividing the installed capacity in an area by the amount of PV installations in that same area. The installed capacity and number of installations are extracted from (Australian Photovoltaic Institute, 2021) for assets declared as “Under 10 kW" following the Australian PV Institutes assumption that assets with a capacity greater than 10 kW are commercial assets.

Values extracted from the Australian PV Institutes are provided on a postcode level. These postcodes are associated with their postal areas. In turn, these postal areas are broken down into their mesh blocks. Whatever Statistical Area Level 3 holds the most mesh block of a single postal area has the postal area assigned to it. The number of installations for each postal area assigned to the same Statistical Area Level 3 are summed up, while P_{PV} is averaged over all postal area assigned to the same Statistical Area Level 3. This assignment of post code areas to Statistical Area Level 3 is used when ever post code data is employed.

Consider the longitude and latitude of a border point as a 2 dimensional vector. Then, two areas are considered to be connected by a road if the euclidean distance between the two closest border points is less than 10^{-4} equating ≈ 10 m.

Travel distances for commutes including at least 2 areas are calculated based on the GPS centre coordinates. The length of commutes taking place within the same suburb are based on census data for people commuting from home to work with in the same suburb (Australian Bureau of Statistics, 2016). Given the provided distribution of travel distances for this kind of commute, the commute length is drawn at random.

Table 1: Area data

Code	Name	Longitude	Latitude	n_a	n_{wo}	n_w	n_{1PPH}	n_{2PPH}	n_{3PPH}	n_{4PPH}	n_{5+PPH}	P_{PV}
20601	Brunswick - Coburg	144.958	-37.756	10584	26297	2125	9514	11934	5722	4824	2063	3.47 kW
20602	Darebin - South	145.007	-37.768	5864	15727	1730	5933	6627	3314	3188	1214	3.52 kW
20603	Essendon	144.914	-37.763	11077	16969	1592	7590	8179	3972	3951	1877	3.69 kW
20604	Melbourne City	144.948	-37.808	63726	10392	422	20645	23073	8019	3651	1617	3.25 kW
20605	Port Phillip	144.955	-37.848	39027	16761	951	17807	17228	5404	3456	1223	3.54 kW
20606	Stonnington - West	145.009	-37.847	23386	12111	514	10883	11275	3285	2031	837	3.90 kW
20607	Yarra	144.997	-37.801	20949	21570	1149	11824	14265	5543	3570	1345	3.27 kW
20701	Boroondara	145.063	-37.819	16619	47772	4405	14474	18561	9565	11328	5924	3.99 kW
20702	Manningham - West	145.135	-37.769	3342	29225	3454	6181	10421	5938	6017	3277	4.09 kW
20703	Whitehorse - West	145.133	-37.828	5064	33365	3220	8984	10836	6547	6778	3506	3.66 kW
20801	Bayside	145.018	-37.942	5877	31795	2931	8560	11076	5322	6894	3176	4.06 kW
20802	Glen Eira	145.045	-37.901	15724	43119	3592	14359	17008	9233	9845	4627	3.86 kW
20803	Kingston	145.101	-38.000	8859	36427	4829	12096	14071	7154	7552	3345	3.81 kW
20804	Stonnington - East	145.055	-37.868	5482	11179	936	4133	4883	2314	2662	1422	3.94 kW
20901	Banyule	145.085	-37.730	3547	41889	4488	10576	14357	7599	8063	3825	3.76 kW
20902	Darebin - North	145.017	-37.721	4048	33170	2267	9394	10984	5895	5177	3010	3.51 kW
20903	Nillumbik - Kinglake	145.310	-37.567	608	18475	4123	3103	6365	3795	5027	2763	4.10 kW
20904	Whittlesea - Wallan	145.075	-37.465	2668	62926	11019	11197	19557	13549	14772	9659	4.28 kW
21001	Keilor	144.867	-37.731	310	20976	2072	4494	6878	3640	3904	2024	3.79 kW
21002	Macedon Ranges	144.698	-37.393	93	8775	2435	1710	3340	1545	2007	1227	4.28 kW
21003	Moreland - North	144.943	-37.712	1841	27009	1829	6939	8164	4632	4266	2858	3.55 kW
21004	Sunbury	144.732	-37.566	1002	11581	2618	2840	4301	2455	2533	1520	4.18 kW
21005	TullamarinekW - Broadmeadows	144.881	-37.614	1487	42563	8418	7342	11624	8923	9928	9540	4.66 kW
21101	Knox	145.261	-37.890	1614	48113	8881	10857	16499	9932	10704	5668	3.84 kW
21102	Manningham - East	145.230	-37.756	131	7431	1538	1266	2454	1368	1932	1232	4.07 kW
21103	Maroondah	145.265	-37.805	1225	38338	4542	9615	12739	6644	6998	3823	3.78 kW
21104	Whitehorse - East	145.188	-37.833	728	20787	2636	4999	6800	3795	4258	2055	3.76 kW
21105	Yarra Ranges	145.550	-37.747	347	48829	8754	10734	17188	8660	9302	5761	3.88 kW
21201	Cardinia	145.573	-38.083	188	28852	5821	5782	9618	5539	6011	4109	4.31 kW
21202	Casey - North	145.312	-38.005	621	36816	8385	7013	11837	7645	9044	6295	4.08 kW
21203	Casey - South	145.308	-38.144	607	41433	13531	7044	12963	9809	11572	8892	4.62 kW
21204	Dandenong	145.180	-37.998	6749	53718	6500	12431	16688	11517	10609	9131	4.07 kW
21205	Monash	145.146	-37.897	8591	52095	6401	11635	18140	11518	12075	6087	3.90 kW
21301	Brimbank	144.797	-37.752	3344	55124	7087	10745	15959	11272	11181	9414	3.63 kW
21302	Hobsons Bay	144.832	-37.855	2823	28802	3241	7697	9864	5340	5317	2641	3.46 kW
21303	Maribyrnong	144.878	-37.795	8852	24672	1687	8120	9935	5377	4660	2389	3.51 kW
21304	MeltonkW - Bacchus Marsh	144.572	-37.683	601	43762	9006	8111	13030	8872	10645	7269	4.12 kW
21305	Wyndham	144.619	-37.887	1919	60752	14151	10515	17876	14694	15029	10477	4.46 kW
21401	Frankston	145.174	-38.135	2034	48288	5800	13310	15970	8307	7789	4308	3.68 kW
21402	Mornington Peninsula	145.035	-38.342	3634	76584	7932	15561	21094	7954	8471	4707	3.94 kW

B Residence Consumption

Residential consumption time series are derived from (CSIRO, 2017), producing consumption values for probability density values of 10%, 50% and 90%. Adding a 0% density for 0 kWh, a normal distribution is fitted using those four value pairs. Results shown in Figure 9 provide the consumption baseline.

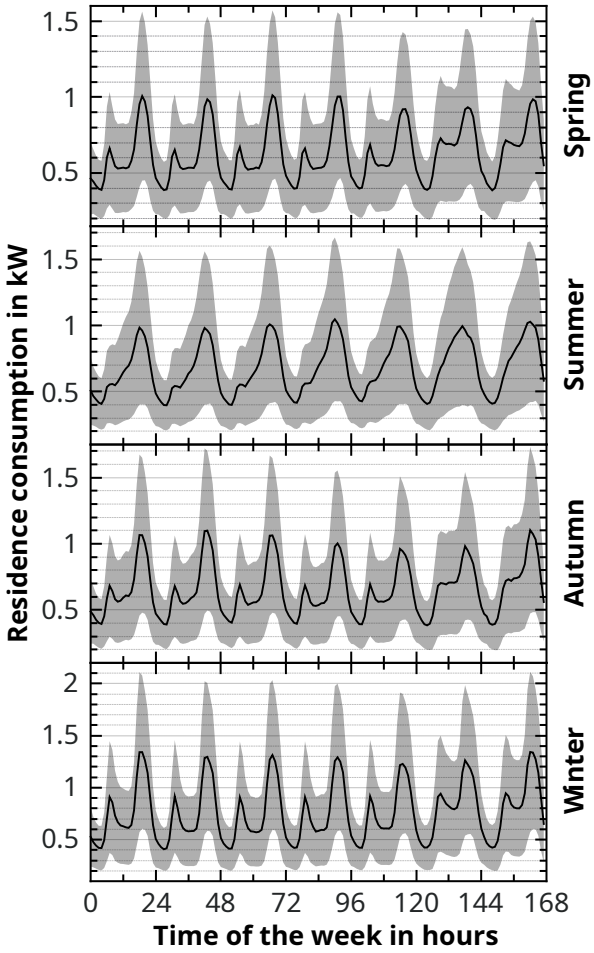

Figure 9: Consumption of dwellings for all seasons. Black lines show the mean of consumption μ_d. Grey areas indicate the interval $[\mu_d - \sigma_d, \mu_d + \sigma_d]$ where σ_d is the standard deviation.

To account for locational consumption deviation δd, data from (Australian Energy Regulator, 2018) is utilised. As this dataset segregates values for several resident groups, the weighted averaged over the population in each considered statistical area is calculated for each season. Parameters needed to build averages: Amount of dwellings with a pool are set to 15%, dwellings heating with gas are set to 43% and dwellings with underfloor

heating are set to 6% (ACIL Allen, 2017) as well as household size as determined above. Results are shown in Table 2

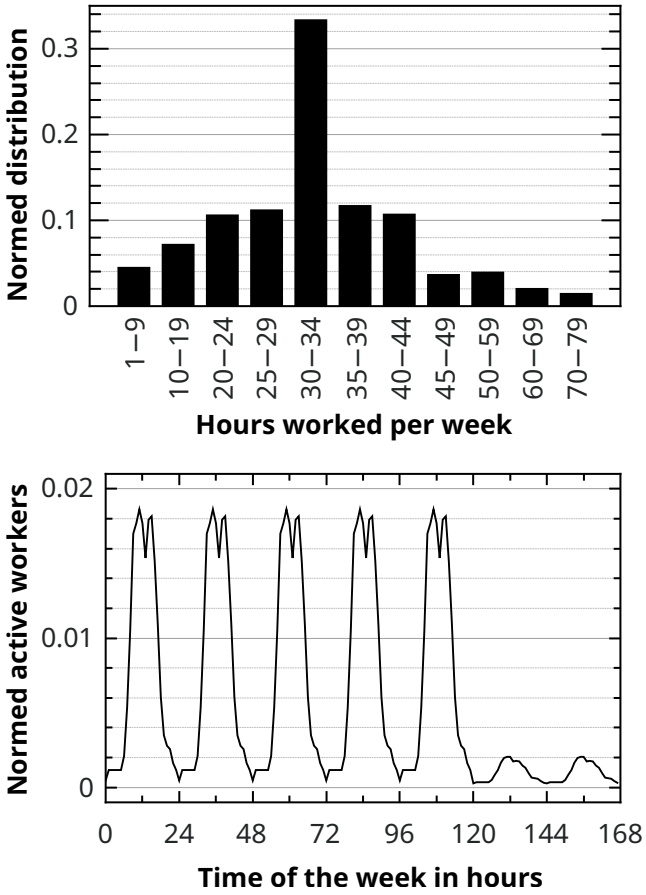

Figure 10: Parameters required for agent scheduling.

C Weather data

Historic data for solar irradiance ϕ_τ and temperature T_τ are provided by Solcast (Solcast, 2019). The dataset contains time series for both variables spanning from the 01.07.2007 00:00:00 Zulu time to 03.03.2021 23:55:00 Zulu time in 5 minute steps. As location the coordinates 37.813628°S, 144.963058°E are selected. For solar irradiance, global tilted irradiance for a fixed angle equalling the latitude is selected. For the temperature, air temperature is selected.

To generate rooftop PV generation forecasts, a historic time series for rooftop PV generation P_τ is calculated using ϕ_τ, T_τ and Equation (1). Denote $\delta t = (24\text{ h})/\Delta t$ and $\gamma = 365 \cdot 12 \cdot \delta t$. Now consider the time steps $\tilde{\tau} \in [0, 365 \cdot 12 \cdot \delta t]$ representing one year.

Table 2: Consumption deviation δd from consumption baseline depending on area, household size and season.

Season:	Spring					Summer					Autumn					Winter				
HHS:	1	2	3	4	5+	1	2	3	4	5+	1	2	3	4	5+	1	2	3	4	5+
Code																				
20601	0.39	0.55	0.61	0.67	0.72	0.39	0.56	0.63	0.69	0.74	0.40	0.56	0.64	0.71	0.76	0.50	0.68	0.80	0.86	0.94
20602	0.39	0.55	0.61	0.67	0.72	0.39	0.56	0.63	0.69	0.74	0.40	0.56	0.64	0.71	0.76	0.50	0.68	0.80	0.86	0.94
20603	0.39	0.55	0.61	0.67	0.72	0.39	0.56	0.63	0.69	0.74	0.40	0.56	0.64	0.71	0.76	0.50	0.68	0.80	0.86	0.94
20604	0.39	0.55	0.61	0.67	0.72	0.39	0.56	0.63	0.69	0.74	0.40	0.56	0.64	0.71	0.76	0.50	0.68	0.80	0.86	0.94
20605	0.39	0.55	0.61	0.67	0.72	0.39	0.56	0.63	0.69	0.74	0.40	0.56	0.64	0.71	0.76	0.50	0.68	0.80	0.86	0.94
20606	0.39	0.55	0.61	0.67	0.72	0.39	0.56	0.63	0.69	0.74	0.40	0.56	0.64	0.71	0.76	0.50	0.68	0.80	0.86	0.94
20607	0.39	0.55	0.61	0.67	0.72	0.39	0.56	0.63	0.69	0.74	0.40	0.56	0.64	0.71	0.76	0.50	0.68	0.80	0.86	0.94
20701	0.39	0.55	0.61	0.67	0.72	0.39	0.56	0.63	0.69	0.74	0.40	0.56	0.64	0.71	0.76	0.50	0.68	0.80	0.86	0.94
20702	0.39	0.55	0.61	0.67	0.72	0.39	0.56	0.63	0.69	0.74	0.40	0.56	0.64	0.71	0.76	0.50	0.68	0.80	0.86	0.94
20703	0.39	0.55	0.61	0.67	0.72	0.39	0.56	0.63	0.69	0.74	0.40	0.56	0.64	0.71	0.76	0.50	0.68	0.80	0.86	0.94
20801	0.39	0.55	0.61	0.67	0.72	0.39	0.56	0.63	0.69	0.74	0.40	0.56	0.64	0.71	0.76	0.50	0.68	0.80	0.86	0.94
20802	0.39	0.55	0.61	0.67	0.72	0.39	0.56	0.63	0.69	0.74	0.40	0.56	0.64	0.71	0.76	0.50	0.68	0.80	0.86	0.94
20803	0.39	0.55	0.61	0.67	0.72	0.39	0.56	0.63	0.69	0.74	0.40	0.56	0.64	0.71	0.76	0.50	0.68	0.80	0.86	0.94
20804	0.39	0.55	0.61	0.67	0.72	0.39	0.56	0.63	0.69	0.74	0.40	0.56	0.64	0.71	0.76	0.50	0.68	0.80	0.86	0.94
20901	0.39	0.55	0.61	0.67	0.72	0.39	0.56	0.63	0.69	0.74	0.40	0.56	0.64	0.71	0.76	0.50	0.68	0.80	0.86	0.94
20902	0.39	0.55	0.61	0.67	0.72	0.39	0.56	0.63	0.69	0.74	0.40	0.56	0.64	0.71	0.76	0.50	0.68	0.80	0.86	0.94
20903	0.39	0.55	0.62	0.67	0.73	0.39	0.56	0.63	0.69	0.74	0.40	0.56	0.64	0.71	0.76	0.51	0.68	0.81	0.86	0.94
20904	0.39	0.56	0.62	0.67	0.74	0.39	0.56	0.63	0.69	0.75	0.41	0.56	0.65	0.71	0.78	0.51	0.69	0.82	0.87	0.96
21001	0.39	0.55	0.61	0.67	0.72	0.39	0.56	0.63	0.69	0.74	0.40	0.56	0.64	0.71	0.76	0.50	0.68	0.80	0.86	0.94
21002	0.44	0.63	0.75	0.75	0.97	0.39	0.55	0.69	0.69	0.85	0.42	0.61	0.73	0.73	0.98	0.60	0.81	0.96	0.96	1.25
21003	0.39	0.55	0.61	0.67	0.72	0.39	0.56	0.63	0.69	0.74	0.40	0.56	0.64	0.71	0.76	0.50	0.68	0.80	0.86	0.94
21004	0.43	0.63	0.74	0.74	0.95	0.39	0.55	0.69	0.69	0.84	0.42	0.61	0.72	0.73	0.96	0.59	0.80	0.95	0.95	1.22
21005	0.39	0.55	0.61	0.67	0.72	0.39	0.56	0.63	0.69	0.74	0.40	0.56	0.64	0.71	0.76	0.50	0.68	0.80	0.86	0.94
21101	0.40	0.57	0.64	0.68	0.78	0.39	0.56	0.64	0.69	0.77	0.41	0.57	0.66	0.71	0.81	0.53	0.71	0.84	0.88	1.01
21102	0.39	0.55	0.61	0.67	0.72	0.39	0.56	0.63	0.69	0.74	0.40	0.56	0.64	0.71	0.76	0.50	0.68	0.80	0.86	0.94
21103	0.39	0.55	0.61	0.67	0.72	0.39	0.56	0.63	0.69	0.74	0.40	0.56	0.64	0.71	0.76	0.50	0.68	0.80	0.86	0.94
21104	0.39	0.55	0.61	0.67	0.72	0.39	0.56	0.63	0.69	0.74	0.40	0.56	0.64	0.71	0.76	0.50	0.68	0.80	0.86	0.94
21105	0.43	0.62	0.72	0.73	0.92	0.39	0.55	0.68	0.69	0.83	0.42	0.60	0.71	0.72	0.94	0.58	0.78	0.93	0.94	1.19
21201	0.39	0.55	0.61	0.67	0.72	0.39	0.56	0.63	0.69	0.74	0.40	0.56	0.64	0.71	0.76	0.50	0.68	0.80	0.86	0.94
21202	0.39	0.55	0.62	0.67	0.73	0.39	0.56	0.63	0.69	0.75	0.41	0.56	0.64	0.71	0.77	0.51	0.68	0.81	0.86	0.95
21203	0.39	0.55	0.61	0.67	0.72	0.39	0.56	0.63	0.69	0.74	0.40	0.56	0.64	0.71	0.76	0.50	0.68	0.80	0.86	0.94
21204	0.39	0.55	0.61	0.67	0.72	0.39	0.56	0.63	0.69	0.74	0.40	0.56	0.64	0.71	0.76	0.50	0.68	0.80	0.86	0.94
21205	0.39	0.55	0.61	0.67	0.72	0.39	0.56	0.63	0.69	0.74	0.40	0.56	0.64	0.71	0.76	0.50	0.68	0.80	0.86	0.94
21301	0.39	0.55	0.61	0.67	0.72	0.39	0.56	0.63	0.69	0.74	0.40	0.56	0.64	0.71	0.76	0.50	0.68	0.80	0.86	0.94
21302	0.39	0.55	0.61	0.67	0.72	0.39	0.56	0.63	0.69	0.74	0.40	0.56	0.64	0.71	0.76	0.50	0.68	0.80	0.86	0.94
21303	0.39	0.55	0.61	0.67	0.72	0.39	0.56	0.63	0.69	0.74	0.40	0.56	0.64	0.71	0.76	0.50	0.68	0.80	0.86	0.94
21304	0.40	0.56	0.64	0.68	0.77	0.39	0.56	0.64	0.69	0.76	0.41	0.57	0.66	0.71	0.80	0.52	0.70	0.83	0.88	1.00
21305	0.39	0.55	0.61	0.67	0.72	0.39	0.56	0.63	0.69	0.74	0.40	0.56	0.64	0.71	0.76	0.50	0.68	0.80	0.86	0.94
21401	0.39	0.55	0.61	0.67	0.72	0.39	0.56	0.63	0.69	0.74	0.40	0.56	0.64	0.71	0.76	0.50	0.68	0.80	0.86	0.94
21402	0.39	0.55	0.61	0.67	0.72	0.39	0.56	0.63	0.69	0.74	0.40	0.56	0.64	0.71	0.76	0.50	0.68	0.80	0.86	0.94

Table 3: Implemented car models

Make	Model	c in $\frac{\text{kWh}}{\text{km}}$	b in kWh	cr^{AC} in kW	cr^{DC} in kW
Hyundai	Ioniq Electric	0.155	38.3	7.2	100
Hyundai	Kona Electric	0.175	64	7.2	100
BMW	i3	0.186	42.2	11	50
Renault	Zoe	0.178	45.6	22	43
Jaguar	I-Pace	0.273	90	7	100
Tesla	Model 3 SR+	0.16	54	11.5	120
Tesla	Model 3 LR	0.174	79.5	11.5	120
Tesla	Model X LR	0.217	100	11.5	225
Telsa	Model S LR	0.189	100	11.5	225
Mercedes Benz	EQC 400 4MATIC	0.216	80	7.4	110
Audi	E-tron 50 quattro	0.224	71	11	120
Audi	E-tron 55 quattro	0.237	95	11	150
Mini Cooper	SE	0.194	32.6	7.4	50
MG	ZS EV	0.186	44.5	7.4	50
Kia	e-Niro	0.186	64	7.2	100
VW	ID.3 Pure	0.161	45	7.2	50
VW	ID.3 Pro	0.166	58	11	100
VW	ID.3 Pro S	0.171	77	11	125
VW	ID.4 Pro	0.172	77	11	125

To create a forecast for a selected $\tilde{\tau}$ unordered tuples $(P_{y\gamma+(\tau-7\cdot\delta t)\%\gamma}, P_{y\gamma+(\tau-6\cdot\delta t)\%\gamma}, \ldots, P_{y\gamma+(\tau+7\cdot\delta t)\%\gamma})$ are created for each recorded year y. Join all these tuples created for $\tilde{\tau}$ to one unordered tuple $H_{\tilde{\tau}}$. Denote $P_{\tilde{\tau}}^{max} = \max H_{\tilde{\tau}}$. Fit the histogram of $H_{\tilde{\tau}}$ using

$$f(x) = y_{\tilde{\tau}} + \frac{A_{\tilde{\tau}}}{\sqrt{2}\pi\sigma_{\tilde{\tau}}} \exp\left(\frac{(x-\mu_{\tilde{\tau}})^2}{2\sigma_{\tilde{\tau}}^2}\right), \tag{C.22}$$

with parameters constraint to $0 \leq A_{\tilde{\tau}} \leq \infty$, $0 \leq y_{\tilde{\tau}} \leq \infty$, $\frac{4}{5}P_{\tilde{\tau}}^{max} \leq \mu_{\tilde{\tau}} \leq P_{\tilde{\tau}}^{max}$

and $0 \leq \sigma_{\tilde{\tau}} \leq \frac{1}{6} P_{\tilde{\tau}}^{max}$. Drop all entries smaller than $x_{\tilde{\tau}}^{b} = \mu_{\tilde{\tau}} - 2\sigma_{\tilde{\tau}}$ from $H_{\tilde{\tau}}$ and fit the resulting histogram using

$$f(x) = \frac{A_{\tilde{\tau}}^{po}}{\sqrt{2}\pi\sigma_{\tilde{\tau}}^{po}} \exp\left(\frac{(x - \mu_{\tilde{\tau}}^{po})^2}{2(\sigma_{\tilde{\tau}}^{po})^2}\right) \tag{C.23}$$

Denote the surface under Equation (C.23) $a_{\tilde{\tau}}$.

Both, $\mu^{PV}(\tilde{\tau}_R, \tilde{\tau}_D)$ and $\sigma^{PV}(\tilde{\tau}_R, \tilde{\tau}_D)$ are determined as follows. For each time step $\hat{\tau} \in [\tilde{\tau}_R, \tilde{\tau}_D)$: If $P_{\tilde{\tau}}^{max} y_{\tilde{\tau}} \leq a_{\tilde{\tau}}$ add $\mu_{\tilde{\tau}}^{po}$ to unorder tuple $\tilde{\mu}$ and $\sigma_{\tilde{\tau}}^{po}$ to unorder tuple $\tilde{\sigma}$. Otherwise, add $P_{\hat{\tau}}^{max}$ to unordered tuple $\tilde{P}^{max}$. Once all $\hat{\tau}$ have been assigned, calculate $\hat{P}^{max}$ to be the sum over all elements in $\tilde{P}^{max}$. Then, use a normal distribution to approximate Irwin-Hall distribution of order $|\tilde{P}^{max}|$ and add resulting mean multiplied by $\hat{P}^{max}$ and standard deviation multiplied by $\hat{P}^{max}$ to $\tilde{\mu}$ and $\tilde{\sigma}$, respectively. Then, $\mu^{PV}(\tilde{\tau}_R, \tilde{\tau}_D)$ is the sum of all elements in $\tilde{\mu}$ and $\sigma^{PV}(\tilde{\tau}_R, \tilde{\tau}_D)$ is the square root over the sum of all squared elements in $\tilde{\sigma}$.

D Derivation of charging quantity

Start with the equation for Conditional Value at Risk for over estimating charging from excess PV at the agent's residence:

$$CVaR_C(q^h) = \min_{\Phi} \Phi + \frac{1}{1-\alpha} \int_{-\infty}^{\infty} \left[f(q^h, Y) - \Phi\right]^+ N(Y, \mu, \sigma) dY, \tag{D.24}$$

with q^h guessing PV excess, α considered percentage of worst cases, normal distribution $N(Y, \mu, \sigma)$ describing the chances to realise q^R with mean μ and standard deviation σ. Define an operator such that $[\circ]^+ = \max(\circ, 0)$. As loss function select

$$f(q^h, Y) = (\Delta p)[q^h - Y]^+, \tag{D.25}$$

with $\Delta p = p^g - p^f$ Then $CVaR_C(q^h)$ can be expressed as

$$CVaR_C(q^h) = \Delta p\Bigg(q^h - \Psi - \mu + \frac{1}{1-\alpha}\left(\frac{\Psi}{2}\left(\operatorname{erf}\left(\frac{\Psi}{\sqrt{2}\sigma}\right)+1\right) + \sigma^2 N(\Psi, 0, \sigma)\right)\Bigg), \tag{D.26}$$

with

$$\Psi = q^h - \mu - [q^h - \mu - \sqrt{2}\sigma \operatorname{erf}^{-1}(1-2\alpha)]^+ \tag{D.27}$$

Neglecting emergency charge amount q^{em}, the charging cost function at work is:

$$\begin{aligned} C(q^w, q^h) = q^w p^w + q^h q^f + ([q^{ow} - soc - q^w]^+ \\ + [q^{ow} - [soc + q^w - q^{ow}]^+ - q^h]^+)p^p + CVaR(q^h) \end{aligned} \tag{D.28}$$

The first derivative of Equation (D.26) is

$$\begin{aligned} &\frac{d}{dq^h} CVaR_C(q^h) \\ &\quad = \Delta p\Bigg(1 + \left(\frac{1}{2(1-\alpha)}\left(\operatorname{erf}\left(\frac{q^h - \mu}{\sqrt{2}\sigma}\right)+1\right) - 1\right)\left(q^h \leq \mu + \sqrt{2}\sigma \operatorname{erf}^{-1}(1-2\alpha)\right)\Bigg) \end{aligned} \tag{D.29}$$

Assume $p^f < p^w < p^g$. Then, minimisation of Equation (D.28) requires $q^h + q^w = 2q^{ow} - soc$. As $q^h \geq 0$ kWh this can be expressed as $q^h = [2q^{ow} - soc - q^w]^+$. With that:

$$\begin{aligned} \frac{d}{dq^w} CVaR_C(q^w) = \Delta p\Bigg(1 + \left(\frac{1}{2(1-\alpha)}\left(\operatorname{erf}\left(\frac{2q^{ow} - soc - q^w - \mu}{\sqrt{2}\sigma}\right)+1\right) - 1\right) \\ \cdot \left(q^w \leq 2q^{ow} - soc - \mu - \sqrt{2}\sigma \operatorname{erf}^{-1}(1-2\alpha)\right)\Bigg)(q^w \leq 2q^{ow} - soc) \end{aligned} \tag{D.30}$$

Thus, the first derivative of Equation (D.28) is

$$\frac{d}{dq^w}C(q^h,q^w) = p^w - p^f - p^p(2q^{ow} > soc + q^w + q^h)$$
$$-\Delta p\left(1+\left(\frac{\operatorname{erf}\left(\frac{2q^{ow}-soc-q^w-\mu}{\sqrt{2}\sigma}\right)+1}{2(1-\alpha)}-1\right)\left(q^w \leq 2q^{ow} - soc - \mu - \sqrt{2}\sigma\operatorname{erf}^{-1}(1-2\alpha)\right)\right)$$
$$\cdot (q^w \leq 2q^{ow} - soc) \quad \text{(D.31)}$$

Then for charging at work in the range of $q^{ow} \leq q^w + soc \leq 2q^{ow}$ and with $2q^{ow} - soc = q^h + q^w$ this can be simplified to

$$\frac{d}{dq^w}C(q^w) = p^w - p^g - \Delta p\left(\left(\frac{1}{2(1-\alpha)}\left(\operatorname{erf}\left(\frac{2q^{ow}-soc-q^w-\mu}{\sqrt{2}\sigma}\right)+1\right)-1\right)\right.$$
$$\left.\cdot\left(q^w \leq 2q^{ow} - soc - \mu - \sqrt{2}\sigma\operatorname{erf}^{-1}(1-2\alpha)\right)\right) \quad \text{(D.32)}$$

Which shows that the minimisation of the charge cost function when charging at work has optimal value

$$q_0^w = \begin{cases} q^{ow} - soc, & \text{if } p^w > p^g \\ \in [q^{ow} - soc, \Xi], & \text{if } p^w = p^g \\ \Xi, & \text{if } p^f < p^w < p^g \\ 2q^{ow} - soc, & \text{if } p^f \geq p^w \end{cases} \quad \text{(D.33)}$$

with

$$\Xi = q^{ow} - soc - \mu - \sqrt{2}\sigma\operatorname{erf}^{-1}\left((1-2\alpha)\left(1-\frac{p^g-p^f}{p^g-p^w}\right)-1\right) \quad \text{(D.34)}$$

E Determination of Agents' schedules

To determine its schedule, the agent first determines the time it spends at work every week. To-do so, the agent draws a time interval from a weighted list representing the distribution of hours worked by Australians per week, compare Figure 10a). From the

drawn time interval, the agent picks at random a natural number representing its weekly worked hours. $\vec{wwh} \in \mathbb{N}^n$ is defined so that the element wwh_i holds the weekly hours worked by the i-th agent, with $twwh = \sum_{i=1}^{n} wwh_i$.

Drawing inspiration from the Fair Work legislation, the maximum shift length an agent may work is set to $masl = 12$ h and the rest period between shifts is set to $rp = 10$ h (AHTS, 2021). The minimum shift length is $misl = 4$ h, which applies to all but one shift an agent works. To schedule the shifts of all agents, $\vec{rt}, \vec{rc} \in \mathbb{R}^{7 \cdot 24}$ are introduced. Element rt_h is the relative target at hour of the week h, that is the ratio between the hours worked on average at the h-th hour of the week and the sum of all hours worked per week, as depicted in Figure 10b). Element rc_h is the relative coverage of hour of the week h, that is the ratio between all agents currently scheduled to work the h-th hour of the week and the hours worked on average at h-th hour of the week. The process of scheduling shifts for each agent is shown in Figure 11.

References

ABS Geospatial Solutions (2020), 'ASGS (2016 Edition) - Boundaries'.

URL: *https://data.gov.au/data/dataset/asgs-2016-edition-boundaries*

ACIL Allen (2017), Energy Consumption Benchmarks Electricity and Gas for Residential Customers, Technical report, ACIL Allen Consulting Pty Ltd, Melbourne, Australia.

Adam Krogh (2021), 'Snazzy Maps - Free Styles for Google Maps'.

URL: *https://snazzymaps.com/editor/customize/237429*

AHTS (2021), 'Employee Rights in Australia'.

URL: *http://ahts.sa.edu.au/employee-rights-in-australia/*

Australian Automobile Association (2019), Road Congestion in Australia, Technical report, Australian Automobile Association, Canberra, ACT, Australia.

URL: *https://www.aaa.asn.au/wp-content/uploads/2019/06/Road-Congestion-In-Australia-2019-v.3.pdf*

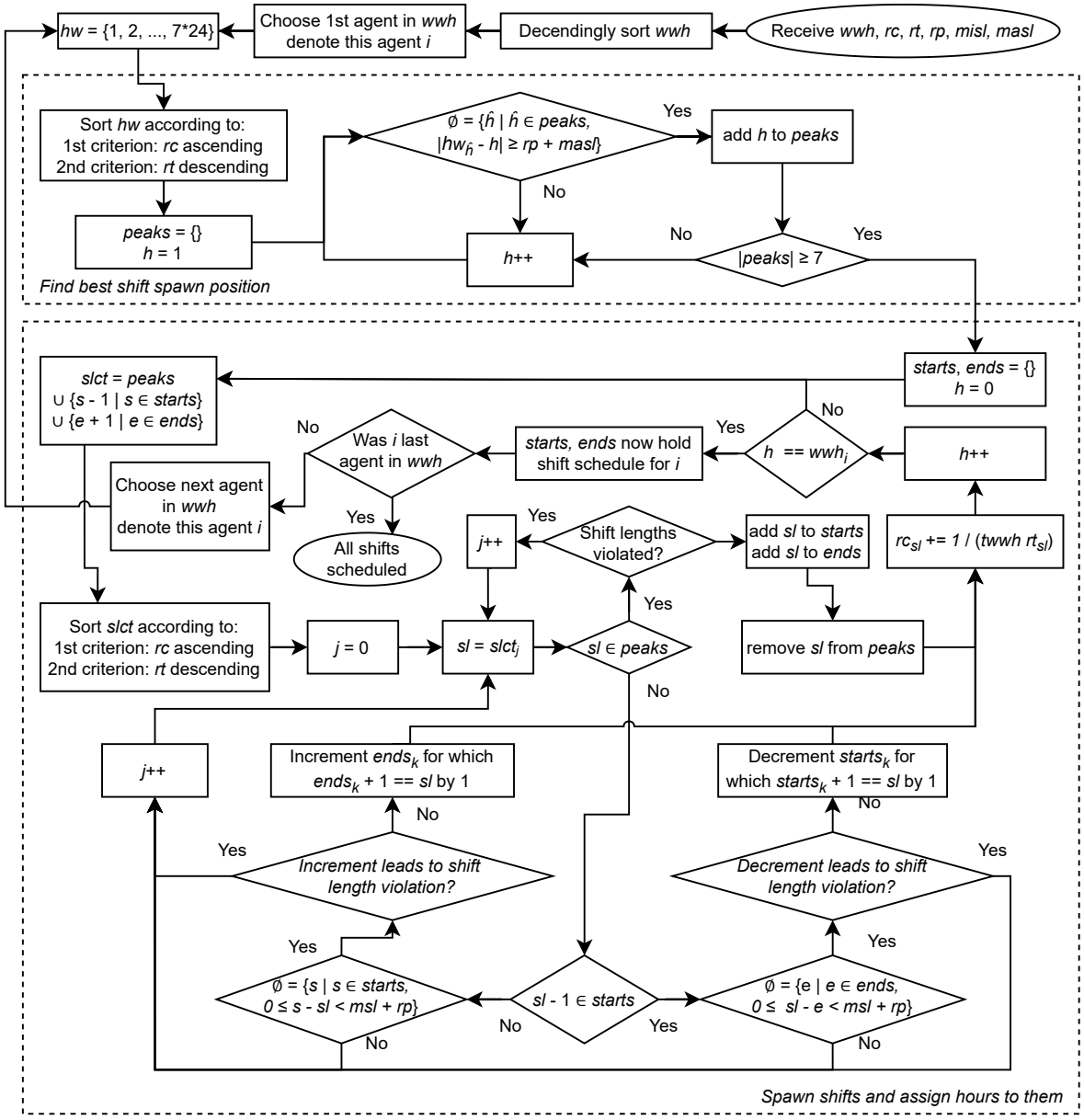

Figure 11: Simplified logic for agent scheduling.

Australian Bureau of Statistics (2016), 'TableBuilder'.

URL: *https://www.abs.gov.au/websitedbs/censushome.nsf/home/tablebuilder*

Australian Energy Regulator (2018), 'Electricity and gas bill benchmarks for residential customers 2017'.

URL: *https://www.aer.gov.au/retail-markets/guidelines-reviews/electricity-and-gas-bill-benchmarks-for-residential-customers-2017*

Australian Photovoltaic Institute (2021), 'Mapping Australian Photovoltaic installations'.

URL: *https://pv-map.apvi.org.au/historical#10/-38.0719/145.0237*

Azadfar, E., Sreeram, V. and Harries, D. (2015), 'The investigation of the major factors influencing plug-in electric vehicle driving patterns and charging behaviour', *Renewable and Sustainable Energy Reviews* **42**(C), 1065–1076. Publisher: Elsevier.
URL: *https://doi.org/10.1016/j.rser.2014.10.058*

Bailey, J., Miele, A. and Axsen, J. (2015), 'Is awareness of public charging associated with consumer interest in plug-in electric vehicles?', *Transportation Research Part D* **36**, 1–9.
URL: *https://doi.org/10.1016/j.trd.2015.02.001*

Bhandari, R. and Stadler, I. (2009), 'Grid parity analysis of solar photovoltaic systems in Germany using experience curves', *Solar Energy* **83**(9), 1634–1644.
URL: *https://doi.org/10.1016/j.solener.2009.06.001*

Bonabeau, E. (2002), 'Agent-based modeling: Methods and techniques for simulating human systems', *Proceedings of the National Academy of Sciences* **99**(suppl 3), 7280–7287.
URL: *https://doi.org/10.1073/pnas.082080899*

Bosetti, V. and Longden, T. (2013), 'Light duty vehicle transportation and global climate policy: The importance of electric drive vehicles', *Energy Policy* **58**, 209–219.
URL: *https://doi.org/10.1016/j.enpol.2013.03.008*

Chaudhari, K., Kandasamy, N. K., Krishnan, A., Ukil, A. and Gooi, H. B. (2019), 'Agent-Based Aggregated Behavior Modeling for Electric Vehicle Charging Load', *IEEE Transactions on Industrial Informatics* **15**(2), 856–868.
URL: *https://doi.org/10.1109/TII.2018.2823321*

Coffman, M., Bernstein, P. and Wee, S. (2017), 'Electric vehicles revisited: a review of factors that affect adoption', *Transport Reviews* **37**(1), 79–93.
URL: *https://doi.org/10.1080/01441647.2016.1217282*

Cranney, K. (2021), 'Australia installs record-breaking number of rooftop solar panels'.

URL: *https://www.csiro.au/en/news/news-releases/2021/australia-installs-record-breaking-number-of-rooftop-solar-panels*

CSIRO (2017), 'Typical House Energy Use'.

URL: *https://ahd.csiro.au/other-data/typical-house-energy-use/*

Dorokhova, M., Martinson, Y., Ballif, C. and Wyrsch, N. (2021), 'Deep reinforcement learning control of electric vehicle charging in the presence of photovoltaic generation', *Applied Energy* **301**(C).

URL: *https://ideas.repec.org/a/eee/appene/v301y2021ics0306261921008874.html*

Essential Services Commission (2021), 'Minimum feed-in tariff | Essential Services Commission'.

URL: *https://www.esc.vic.gov.au/electricity-and-gas/electricity-and-gas-tariffs-and-benchmarks/minimum-feed-tariff*

Feldman, D., Ramasamy, V., Fu, R., Ramdas, A., Desai, J. and Margolis, R. (2021), U.S. Solar Photovoltaic System and Energy Storage Cost Benchmark: Q1 2020, Technical Report NREL/TP-6A20-77324, National Renewable Energy Laboratory.

Fetene, G. M., Hirte, G., Kaplan, S., Prato, C. G. and Tscharaktschiew, S. (2016), 'The economics of workplace charging', *Transportation Research Part B: Methodological* **88**, 93–118.

URL: *https://doi.org/10.1016/j.trb.2016.03.004*

Funke, S. A., Sprei, F., Gnann, T. and Plötz, P. (2019), 'How much charging infrastructure do electric vehicles need? A review of the evidence and international comparison', *Transportation Research Part D: Transport and Environment* **77**, 224–242.

URL: *https://doi.org/10.1016/j.trd.2019.10.024*

Google Australia Pty Ltd (2021), 'Google Maps'.

URL: *https://www.google.com.au/maps/@-38.0804825,144.8906867,10z*

Hardman, S., Jenn, A., Tal, G., Axsen, J., Beard, G., Daina, N., Figenbaum, E., Jakobsson, N., Jochem, P., Kinnear, N., Plötz, P., Pontes, J., Refa, N., Sprei, F., Turrentine,

T. and Witkamp, B. (2018), 'A review of consumer preferences of and interactions with electric vehicle charging infrastructure', *Transportation Research Part D: Transport and Environment* **62**.
URL: *https://doi.org/10.1016/j.trd.2018.04.002*

Higashitani, T., Ikegami, T., Uemichi, A. and Akisawa, A. (2021), 'Evaluation of residential power supply by photovoltaics and electric vehicles', *Renewable Energy* **178**, 745–756.
URL: *https://doi.org/10.1016/j.renene.2021.06.097*

Huang, Y. and Zhou, Y. (2015), 'An optimization framework for workplace charging strategies', *Transportation Research Part C: Emerging Technologies* **52**, 144–155.
URL: *https://doi.org/10.1016/j.trc.2015.01.022*

IEA (2019), Global EV Outlook 2019, Technical report, IEA, Paris, France.
URL: *https://www.iea.org/reports/global-ev-outlook-2019*

IEA (2020), Tracking Transport 2020, Technical report, IEA, Paris, France.
URL: *https://www.iea.org/reports/tracking-transport-2020*

IEA (2021), Global EV Outlook 2021, Technical report, IEA, Paris, France.
URL: *https://www.iea.org/reports/global-ev-outlook-2021*

JOLT Charge Pty Ltd. (2021), 'How Much Does it Cost to Charge an Electric Vehicle in Australia'.
URL: *https://jolt.com.au/cost-to-charge-electric-vehicle*

Kalghatgi, G. (2018), 'Is it really the end of internal combustion engines and petroleum in transport?', *Applied Energy* **225**, 965–974.
URL: *https://doi.org/10.1016/j.apenergy.2018.05.076*

Kazil, J., Masad, D. and Crooks, A. (2020), Utilizing Python for Agent-Based Modeling: The Mesa Framework, *in* R. Thomson, H. Bisgin, C. Dancy, A. Hyder and M. Hussain, eds, 'Social, Cultural, and Behavioral Modeling', Lecture Notes in Computer Science,

Springer International Publishing, Cham, pp. 308–317.
URL: *https://doi.org/10.1007/978-3-030-61255-9_30*

Knobloch, F., Hanssen, S. V., Lam, A., Pollitt, H., Salas, P., Chewpreecha, U., Huijbregts, M. A. J. and Mercure, J.-F. (2020), 'Net emission reductions from electric cars and heat pumps in 59 world regions over time', *Nature Sustainability* **3**(6), 437–447.
URL: *https://doi.org/10.1038/s41893-020-0488-7*

Langbroek, J. H. M., Franklin, J. P. and Susilo, Y. O. (2016), 'The effect of policy incentives on electric vehicle adoption', *Energy Policy* **94**, 94–103.
URL: *https://doi.org/10.1016/j.enpol.2016.03.050*

Lieven, T. (2015), 'Policy measures to promote electric mobility – A global perspective', *Transportation Research Part A: Policy and Practice* **82**, 78–93.
URL: *https://doi.org/10.1016/j.tra.2015.09.008*

Matthews, L., Lynes, J., Riemer, M., Del Matto, T. and Cloet, N. (2017), 'Do we have a car for you? Encouraging the uptake of electric vehicles at point of sale', *Energy Policy* **100**, 79–88.
URL: *https://doi.org/10.1016/j.enpol.2016.10.001*

Millo, F., Rolando, L., Fuso, R. and Mallamo, F. (2014), 'Real CO2 emissions benefits and end user's operating costs of a plug-in Hybrid Electric Vehicle', *Applied Energy* **114**, 563–571.
URL: *https://doi.org/10.1016/j.apenergy.2013.09.014*

Mountain, B. (2017), The retail electricity market for households and small businesses in Victoria: Analysis of offers and bills, Monograph, Victoria University, Melbourne, Australia.
URL: *https://www.energy.vic.gov.au/__data/assets/pdf_file/0030/79158/CME-electricity-analysis-of-offers-and-bills-July-2017.pdf*

Nicholas, M. (2019), Estimating electric vehicle charging infrastructure costs across major U.S. metropolitan areas, Working paper, The International Concil on Clean

Transportation.
URL: *https://theicct.org/sites/default/files/publications/ICCT_EV_Charging_Cost_20190813.pdf*

Nilsson, M. and Nykvist, B. (2016), 'Governing the electric vehicle transition – Near term interventions to support a green energy economy', *Applied Energy* **179**(C), 1360–1371.
URL: *https://doi.org/10.1016/j.apenergy.2016.03.056*

Parkinson, G. (2020), 'Tesla lifts Supercharging rate in Australia to 52c/kWh'.
URL: *https://reneweconomy.com.au/tesla-lifts-supercharging-rate-in-australia-to-52c-kwh-88039/*

Pietzcker, R. C., Longden, T., Chen, W., Fu, S., Kriegler, E., Kyle, P. and Luderer, G. (2014), 'Long-term transport energy demand and climate policy: Alternative visions on transport decarbonization in energy-economy models', *Energy* **64**, 95–108.
URL: *https://doi.org/10.1016/j.energy.2013.08.059*

Schneider, C. M., Belik, V., Couronné, T., Smoreda, Z. and González, M. C. (2013), 'Unravelling daily human mobility motifs', *Journal of The Royal Society Interface* **10**(84), 1–8. Publisher: Royal Society.
URL: *https://doi.org/10.1098/rsif.2013.0246*

Solcast (2019), 'Global solar irradiance data and PV system power output data'.
URL: *https://solcast.com/*

van der Meer, D., Chandra Mouli, G. R., Morales-España Mouli, G., Elizondo, L. R. and Bauer, P. (2018), 'Energy Management System With PV Power Forecast to Optimally Charge EVs at the Workplace', *IEEE Transactions on Industrial Informatics* **14**(1), 311–320. Conference Name: IEEE Transactions on Industrial Informatics.
URL: *https://doi.org/10.1109/TII.2016.2634624*

Williams, B. and DeShazo, J. R. (2014), 'Pricing Workplace Charging: Financial Viability and Fueling Costs', *Transportation Research Record* **2454**(1), 68–75.
URL: *https://doi.org/10.3141/2454-09*